Continuum Mech. Thermodyn. (2017) 29:535–557
DOI 10.1007/s00161-016-0544-8

ORIGINAL ARTICLE

Felix A. Reich · Wilhelm Rickert · Oliver Stahn · Wolfgang H. Müller

Magnetostriction of a sphere: stress development during magnetization and residual stresses due to the remanent field

Received: 25 May 2016 / Accepted: 24 November 2016 / Published online: 28 December 2016

Abstract Based on the principles of rational continuum mechanics and electrodynamics (see Truesdell and Toupin in Handbuch der Physik, Springer, Berlin, 1960 or Kovetz in Electromagnetic theory, Oxford University Press, Oxford, 2000), we present closed-form solutions for the mechanical displacements and stresses of two different magnets. Both magnets are initially of spherical shape. The first (hard) magnet is uniformly magnetized and deforms due to the field induced by the magnetization. In the second problem of a (soft) linear-magnetic sphere, the deformation is caused by an applied external field, giving rise to magnetization. Both problems can be used for modeling parts of general magnetization processes. We will address the similarities between both settings in context with the solutions for the stresses and displacements. In both problems, the volumetric LORENTZ force density vanishes. However, a LORENTZ surface traction is present. This traction is determined from the magnetic flux density. Since the obtained displacements and stresses are small in magnitude, we may use HOOKE'S law with a small-strain approximation, resulting in the LAMÉ-NAVIER equations of linear elasticity theory. If gravity is neglected and azimuthal symmetry is assumed, these equations can be solved in terms of a series. This has been done by HIRAMATSU and OKA (Int J Rock Mech Min Sci Geomech Abstr 3(2):89–90, 1966) before. We make use of their series solution for the displacements and the stresses and expand the LORENTZ tractions of the analyzed problems suitably in order to find the expansion coefficients. The resulting algebraic system yields finite numbers of nonvanishing coefficients. Finally, the resulting stresses, displacements, principal strains and the LORENTZ tractions are illustrated and discussed.

Keywords Magnetostriction · Closed-form solution · Spherical magnets · Linear-elastic

List of symbols

General quantities

$\boldsymbol{v}$	Barycentric velocity (m/s)
$\boldsymbol{v}_I$	Barycentric surface velocity (m/s)
$\boldsymbol{w}$	Velocity of a singular surface (m/s)
$w_\perp$	Normal velocity of a singular surface (m/s)
$\boldsymbol{n}$	Normal vector (1)
P_n	nth Legendre polynomial (1)
R	Radius of the magnetic sphere (m)

Communicated by Andreas Öchsner.

F. A. Reich (✉) · W. Rickert · O. Stahn · W. H. Müller
Institut für Mechanik, Kontinuumsmechanik und Materialtheorie, Technische Universität Berlin, Sek. MS. 2, Einsteinufer 5, 10587 Berlin, Germany
E-mail: felix.reich@tu-berlin.de

r	Radial spherical coordinate (m)
$\tilde{r}$	Dimensionless radial spherical coordinate, $\tilde{r} = r/R$ (1)
ϑ	Polar spherical angle, $\vartheta \in [0, \pi]$ (1)
x	Cosine of polar spherical angle (1)
ξ	Radial cylindrical coordinate (m)
$\tilde{\xi}$	Dimensionless radial cylindrical coordinate, $\tilde{\xi} = \xi/R$ (1)
z	Axial cylindrical coordinate (m)
$\tilde{z}$	Dimensionless axial cylindrical coordinate, $\tilde{z} = z/R$ (1)
φ	Azimuthal angle, $\varphi \in [0, 2\pi)$ (1)
$\boldsymbol{u}$	Displacement vector (m)
u_r	Radial displacement component w.r.t. $\boldsymbol{e}_r$ (m)
u_ϑ	Polar displacement component w.r.t. $\boldsymbol{e}_\vartheta$ (m)
u_φ	Azimuthal displacement component w.r.t. $\boldsymbol{e}_\varphi$ (m)
$(\cdot)^{\mathrm{I}}$	Interior of magnet
$(\cdot)^{\mathrm{E}}$	Exterior of magnet
$(\cdot)^{(\mathrm{I})}$	Problem of uniformly magnetized sphere
$(\cdot)^{(\mathrm{II})}$	Problem of linear-magnetic sphere
$\tilde{(\cdot)}$	A normalized dimensionless function (1)
$\{\boldsymbol{e}_i\}$	Local orthonormal basis, $i \in \{r, \vartheta, \varphi\}$ (1)
$\boldsymbol{e}_z$	Cylindrical axial unit vector (1)
$\boldsymbol{e}_\xi$	Cylindrical radial unit vector (1)
$\mathbf{1}$	Unit tensor, $\mathbf{1} = \sum_{i=1}^{3} \boldsymbol{e}_i \otimes \boldsymbol{e}_i$ (1)
$\mathbf{1}_I$	Interface projector, $\mathbf{1}_I = \mathbf{1} - \boldsymbol{n} \otimes \boldsymbol{n}$ (1)
δ_{ij}	KRONECKER delta (1)
∇	Nabla operator, $\nabla = \boldsymbol{e}_r \frac{\partial}{\partial r} + \boldsymbol{e}_\vartheta \frac{1}{r} \frac{\partial}{\partial \vartheta} + \boldsymbol{e}_\varphi \frac{1}{r \sin\vartheta} \frac{\partial}{\partial \varphi}$ (1/m)
∇_I	Surface nabla, $\nabla_I = \mathbf{1}_I \cdot \nabla$ (1/m)
H	Mean curvature, $H = -\frac{1}{2} \nabla_I \cdot \boldsymbol{n}$ (1/m)

Mechanics

$\boldsymbol{\sigma}$	Cauchy stress tensor (N/m^2)
$\boldsymbol{\sigma}_I$	Cauchy surface stress tensor (N/m)
σ_{ij}	Components of $\boldsymbol{\sigma}$ w.r.t. $\{\boldsymbol{e}_i \otimes \boldsymbol{e}_j\}$, $i, j \in \{r, \vartheta, \varphi\}$ (N/m^2)
σ_{vM}	Equivalent VON MISES stress (N/m^2)
$\boldsymbol{\varepsilon}$	Linear strain tensor (1)
ε_{ij}	Components of $\boldsymbol{\varepsilon}$ w.r.t. $\{\boldsymbol{e}_i \otimes \boldsymbol{e}_j\}$, $i, j \in \{r, \vartheta, \varphi\}$ (1)
Λ_i	A principal strain value, $i \in \{1, 2, 3\}$ (1)
ρ	Mass density (kg/m^3)
ρ_I	Surface mass density (kg/m^2)
λ	LAMÉ's first parameter (N/m^2)
μ	LAMÉ's second parameter (N/m^2)

Electrodynamics

$\boldsymbol{B}$	Magnetic flux density (T)
$\mathfrak{H}$	Potential of free electric current (A/m)
$\mathfrak{H}_0$	Amplitude of an external field $\mathfrak{H}$ (A/m)
V_{m}	A potential of $\mathfrak{H}$, where $\mathfrak{H} = -\nabla V_{\mathrm{m}}$ (A)
$\mathfrak{D}$	Potential of free electric charge (C/m^2)
$\boldsymbol{E}$	Electric field (N/C)
$\boldsymbol{M}$	MINKOWSKI magnetization (A/m)
M_0	Strength of the magnet's uniform magnetization (A/m)
$\boldsymbol{P}$	Polarization (C/m^2)
μ_0	Vacuum permeability (N/A^2)
μ_{r}	Relative permeability (1)

ϵ_0	Vacuum permittivity ($\mathrm{A^2 s^2/(N\,m^2)}$)
q	Total electric charge density ($\mathrm{C/m^3}$)
q^{f}	Free electric charge density ($\mathrm{C/m^3}$)
q^{r}	Bound electric charge density ($\mathrm{C/m^3}$)
q_I^{f}	Singular free electric charge density ($\mathrm{C/m^2}$)
q_I^{r}	Singular bound electric charge density ($\mathrm{C/m^2}$)
$\boldsymbol{J}$	Total electric current density ($\mathrm{A/m^2}$)
$\boldsymbol{J}^{\mathrm{f}}$	Free electric current density ($\mathrm{A/m^2}$)
$\boldsymbol{J}^{\mathrm{r}}$	Bound electric current density ($\mathrm{A/m^2}$)
$\boldsymbol{J}_I$	Singular total electric current density (A/m)
$\boldsymbol{J}_I^{\mathrm{f}}$	Singular free electric current density (A/m)
$\boldsymbol{J}_I^{\mathrm{r}}$	Singular bound electric current density (A/m)
$\boldsymbol{j}^{\mathrm{f}}$	Free diffusive electric current density ($\mathrm{A/m^2}$)
$\boldsymbol{j}_I^{\mathrm{f}}$	Singular free diffusive electric current density (A/m)

Mixed mechanics and electrodynamics

$\boldsymbol{f}^{\mathrm{L}}$	Volumetric LORENTZ force density ($\mathrm{N/m^3}$)
$\boldsymbol{f}_I^{\mathrm{L}}$	Surface LORENTZ force density ($\mathrm{N/m^2}$)

1 Introduction

In certain materials, mechanical strains and stresses can be induced by electromagnetic coupling. The special case of deformation of magnetic media due to a magnetic field is often referred to as magnetostriction. In commercial (hard) permanent magnets, this effect, which is due to their own remanent electromagnetic field, is relatively small and therefore often neglected. Nevertheless, for a representative case, it is our goal to determine the magnitude of the eigenstresses as well as the size and the shape of deformation in order to validate this assumption. Furthermore, in (soft) linear magnets stresses can be induced by external fields. Here, the mechanical stresses vary with the externally applied field. For real magnets, both problems are relevant. Figure 1 illustrates that the initial magnetization curve can be approximated by a linear-magnetic model, which is valid up to certain magnitudes of the magnetic field. Therefore, one can employ this model in order to compute strains and stresses for that part of the magnetization process. Once the point of magnetic saturation is reached, there may remain a magnetic flux—even if the external magnetization field is deactivated. This is referred to as the remanent field, which can be modeled by a constant uniform magnetization. Because of the relevance of soft and hard magnets in technical applications we analyze both problems for a similar geometry.

We start by analyzing the eigenstresses of an uniformly magnetized body, which has the form of an ideal sphere before magnetization. The magnetic flux density due to the body's magnetization causes a LORENTZ force density on the surface of the sphere. Thus, deformation and eigenstresses are induced, which are small so that

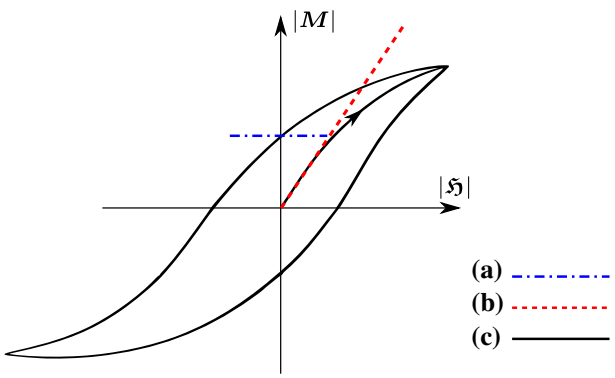

Fig. 1 Comparison of magnetization models. The line (*a*) denotes a remanent uniform constant magnetization, (*b*) represents a linear isotropic magnetization model, and (*c*) shows a real hysteresis loop with initial magnetization curve. Magnets that are modeled by (*a*) or (*b*) are referred to as *hard* and *soft* magnets, respectively

we can work with linearized strains in combination with HOOKE'S law. Later we will examine the deformation and stresses of a linear-magnetic sphere due to an uniform external magnetic field. From a mathematical point of view, the magnetic fields in both problems are closely related, see [7, Sect. 5.11] and we shall reveal further similarities for both stresses and displacements w.r.t. the two considered magnetic problems.

As shown in [5], the LORENTZ surface force density in these problems can be calculated from the jump of the magnetization and the average of the magnetic flux density on the magnet's surface. The solution for the magnetic flux density of a uniformly magnetized sphere is well known, cf. [4,7,16]. We briefly restate a solution method based on a series expansion in order to show similarities in the algebraic structure w.r.t. the mechanical problem.

The elastic problem in spherical coordinates under the assumption of azimuthal symmetry and vanishing body forces was solved analytically by HIRAMATSU and OKA in terms of a series expansions containing LEGENDRE polynomials, see [6]. The authors used their method to analyze tensile strengths of rocks, loaded with uniform pressure in small regions centered around the poles. The method is employed in many other applications with spherical bodies. For example, in [11] the effect of equatorial pressure loads was analyzed and in [18] a hollow internally pressurized sphere was investigated, which, in addition was loaded by an outer pressure at regions around the poles. However, in the magnetic problems in this paper, there is no uniform pressure loading.

In the problem of a uniformly magnetized sphere, the LORENTZ traction has a radial as well as a polar component, which both depend on the polar angle. In order to specialize the elastic solution to the boundary conditions of this problem, we investigate the jump condition of linear momentum in combination with the series solution of HIRAMATSU and OKA. The dependence of the radial stress σ_{rr} on the polar angle is given by LEGENDRE polynomials. Consequently, the radial component of the LORENTZ traction is expanded in a FOURIER-LEGENDRE series. However, the dependence of the shear stress $\sigma_{r\vartheta}$ on the polar angle is given in terms of derivatives of the LEGENDRE polynomials. Therefore, we modify the FOURIER-LEGENDRE series technique and expand the polar traction component by employing derivatives of LEGENDRE polynomials as well. The same can be said for the case of a linear-magnetic sphere in a uniform external field.

It is shown that the FOURIER-LEGENDRE expansions of the force components are finite. Hence, the jump conditions of linear momentum directly yield finite sums for the displacements as well. The resulting closed-form solutions for the displacements and for the stresses are discussed.

Similar problems have been investigated in the literature. For example, in [1, Sect. 10.4] the strains in a magnetized sphere were studied. However, a purely radial surface traction was obtained. Therefore, the author obtained a spherically symmetric problem, which he solved by a technique outlined in [9, Sect. 173]. Another noteworthy examination is given by [3, Sect. 8.4]. The authors study a spherical cavity, which is also uniformly magnetized, and surrounded by a non-permeable medium. They found a traction with nonvanishing radial and polar components, similar to the results presented in this paper. However, they refrained from solving the elastic problem. Furthermore, [12] examined deformation in ellipsoidal and spherical ferrogel samples due to an uniform magnetic field. The authors also obtained a purely radial surface traction and solved their problem analytically in cylindrical coordinates.

In the literature, the magnetic traction is often defined in terms of the normal component of the MAXWELL stress tensor at a surface. The definition of this tensor is based upon an identity of the volumetric LORENTZ force. In this paper, the MAXWELL stress concept is not directly applied, because of various problems, which were detailed in [13]. Rather the explicit LORENTZ force densities for regular and singular points are used, as it was recently explained in [5, Sect. 3.2.3]. In the discussed problems, the volumetric force densities vanish, whereas surface densities remain. Physically, these forces are induced in a very thin volumetric region, i.e., at the surfaces of the magnets. In this region, the magnetization is characterized by steep gradients. As these regions cannot be resolved in a large-scale continuous solution, they are modeled using the mathematical concept of singular surfaces.

2 Governing equations and constitutive laws

In this section, we briefly state the governing equations for our problems. We start with the electromagnetic constitutive equations and proceed by combining them with the electromagnetic equations in the stationary case. The employed electromagnetic force model is examined in context of the problems. The obtained force densities serve as momentum sources in the balance of linear momentum, which is analyzed for both problems in what follows.

2.1 Electromagnetic constitutive equations

In ideal magnets, there are no polarization and no regular and singular free charge density, i.e., $\boldsymbol{P} = \boldsymbol{0}$, $q^{\mathrm{f}} = 0$, and $q_I^{\mathrm{f}} = 0$, respectively. There are no conductible contacts to the spheres; therefore, the regular and singular free diffusive electric current densities also vanish, $\boldsymbol{j}^{\mathrm{f}} = \boldsymbol{0}$ and $\boldsymbol{j}_I^{\mathrm{f}} = \boldsymbol{0}$. The media outside the spheres are assumed to possess no electromagnetic properties, so that all of the aforementioned fields vanish. The surfaces of the magnets still constitute jump surfaces, albeit without intrinsic properties. The differences in both considered problems w.r.t. the magnetic behavior are:

Problem I: Uniformly magnetized sphere The magnetization in the case of the uniformly magnetized sphere is the solenoidal field $\boldsymbol{M}_{(\mathrm{I})} = M_0 \boldsymbol{e}_z$, where $M_0 = \text{const}$.

Problem II: Linear-magnetic sphere In the problem of a linear magnet, we have the relation $\boldsymbol{B} = \mu_0 \mu_{\mathrm{r}} \mathfrak{H}$ in the interior. As it will be shown, the magnetization $\boldsymbol{M}_{(\mathrm{II})}$ in that problem is uniform, if the externally applied field is uniform and solenoidal.

2.2 Electromagnetic field equations

In stationary problems of bodies at rest MAXWELL'S equations reduce to

$$\nabla \times \boldsymbol{E} = \boldsymbol{0}, \quad \epsilon_0 \nabla \cdot \boldsymbol{E} = q^{\mathrm{f}} - \nabla \cdot \boldsymbol{P}, \quad \boldsymbol{n} \times [\![\boldsymbol{E}]\!] = \boldsymbol{0}, \quad \epsilon_0 \boldsymbol{n} \cdot [\![\boldsymbol{E}]\!] = q_I^{\mathrm{f}} - \boldsymbol{n} \cdot [\![\boldsymbol{P}]\!] \tag{2.1}$$

for the electrical problem and to

$$\nabla \times \mathfrak{H} = \boldsymbol{j}^{\mathrm{f}}, \quad \nabla \cdot \mathfrak{H} = -\nabla \cdot \boldsymbol{M}, \quad \boldsymbol{n} \times [\![\mathfrak{H}]\!] = \boldsymbol{j}_I^{\mathrm{f}}, \quad \boldsymbol{n} \cdot [\![\mathfrak{H}]\!] = -\boldsymbol{n} \times [\![\boldsymbol{M}]\!] \tag{2.2}$$

for the magnetic problem. For an overview of the full equations and the used operators see Appendix A. We note that, because of the constitutive relations, the first set of equations reduces in both problems to

$$\nabla \times \boldsymbol{E} = \boldsymbol{0}, \quad \nabla \cdot \boldsymbol{E} = 0\,, \quad \boldsymbol{n} \times [\![\boldsymbol{E}]\!] = \boldsymbol{0}, \quad \boldsymbol{n} \cdot [\![\boldsymbol{E}]\!] = 0. \tag{2.3}$$

There are no sources in these equations. Hence, the electric field vanishes everywhere, i.e., $\boldsymbol{E} = \boldsymbol{0}$, independently of the magnetization. As we shall see there are some differences in the magnetic behavior depending on the case. Nevertheless, note that the magnetization of both problems is solenoidal and uniform. Therefore, the equations of magnetism reduce to

$$\nabla \times \mathfrak{H} = \boldsymbol{0}, \quad \nabla \cdot \mathfrak{H} = 0, \quad \boldsymbol{n} \times [\![\mathfrak{H}]\!] = \boldsymbol{0}, \quad \boldsymbol{n} \cdot [\![\mathfrak{H}]\!] = -\boldsymbol{n} \times [\![\boldsymbol{M}]\!] \tag{2.4}$$

for both problems analyzed.

2.3 Electromagnetic forces

We make use of the LORENTZ force model detailed in Appendix B. In both problems, we have $\nabla \times \boldsymbol{M} = \boldsymbol{0}$. With the other constitutive relations, the LORENTZ volume force density becomes:

$$\boldsymbol{f}^{\mathrm{L}} = q\boldsymbol{E} + \boldsymbol{J} \times \boldsymbol{B} = \left(q^{\mathrm{f}} - \nabla \cdot \boldsymbol{P}\right) \boldsymbol{E} + \left(q^{\mathrm{f}} \boldsymbol{v} + \boldsymbol{j}^{\mathrm{f}} + \frac{\partial \boldsymbol{P}}{\partial t} + \nabla \times \boldsymbol{M}\right) \times \boldsymbol{B} = \boldsymbol{0}, \tag{2.5}$$

i.e., there are no electromagnetic body forces in both problems. However, the LORENTZ surface force density does not vanish:

$$\begin{aligned} \boldsymbol{f}_I^{\mathrm{L}} &= q_I \langle \boldsymbol{E} \rangle + \boldsymbol{J}_I \times \langle \boldsymbol{B} \rangle \\ &= (q_I^{\mathrm{f}} - \boldsymbol{n} \cdot [\![\boldsymbol{P}]\!]) \langle \boldsymbol{E} \rangle + (q_I^{\mathrm{f}} \boldsymbol{v}_I + \boldsymbol{j}_I^{\mathrm{f}} - w_\perp [\![\boldsymbol{P}]\!] + \boldsymbol{n} \times [\![\boldsymbol{M}]\!]) \times \langle \boldsymbol{B} \rangle \\ &= (\boldsymbol{n} \times [\![\boldsymbol{M}]\!]) \times \langle \boldsymbol{B} \rangle\,. \end{aligned} \tag{2.6}$$

This density gives rise to elastic deformations.

2.4 Mechanical problem of elasticity

On the mechanical side, we start from the stationary balance of linear momentum. We neglect gravitational forces $\rho \boldsymbol{f}$. Then we have in regular points:

$$\nabla \cdot \boldsymbol{\sigma} = \mathbf{0} \tag{2.7}$$

and jump conditions for points on the boundary of the sphere (singular interface):

$$\boldsymbol{n} \cdot [\![\boldsymbol{\sigma}]\!] = -\boldsymbol{f}_I^{\mathrm{L}}. \tag{2.8}$$

The magnetization in the uniformly magnetized sphere is axial. Hence, it would be consistent to assume transversal isotropic material behavior. However, we assume the deviation from purely isotropic behavior to be negligibly small, cf. [1, Sect. 10.4]. In the other case, the linear-magnetic sphere is isotropic in its magnetization—here the assumption of isotropic elastic behavior is not in contradiction to the magnetization model. Moreover, we put $\boldsymbol{\sigma} = \mathbf{0}$ in the exterior and employ HOOKE'S law for isotropic media with the assumption of small strains, i.e.,

$$\boldsymbol{\sigma} = \lambda \operatorname{tr}(\boldsymbol{\varepsilon})\mathbf{1} + 2\mu\boldsymbol{\varepsilon}, \qquad \text{where} \qquad \boldsymbol{\varepsilon} = \tfrac{1}{2}[\nabla \otimes \boldsymbol{u} + \boldsymbol{u} \otimes \nabla]. \tag{2.9}$$

Both problems are free of body forces and possess azimuthal symmetry. For spherical problems of linear elasticity in this setting, it is convenient to make use of the analytical solution by HIRAMATSU and OKA.

3 The method of Hiramatsu and Oka

For the considered problems, we directly obtain the LAMÉ-NAVIER equations in the form:

$$(\lambda + \mu)\nabla(\nabla \cdot \boldsymbol{u}) + \mu \Delta \boldsymbol{u} = \mathbf{0}. \tag{3.1}$$

The problems are azimuthally symmetric, and there is no azimuthal loading. Consequently, we choose the following semi-inverse *ansatz* for the displacements:

$$\boldsymbol{u}(r, \vartheta) = u_r(r, \vartheta)\boldsymbol{e}_r + u_\vartheta(r, \vartheta)\boldsymbol{e}_\vartheta, \tag{3.2}$$

where $\{\boldsymbol{e}_r, \boldsymbol{e}_\vartheta, \boldsymbol{e}_\varphi\}$ is a local, spherical, orthonormal base. This problem of elasticity in spherical coordinates has been solved by HIRAMATSU and OKA [6] before. Their solution for the displacements and stresses is given in terms of a series containing LEGENDRE polynomials, $P_n(\cos\vartheta)$. Here, the components of the stress tensor are obtained from $\boldsymbol{\sigma} = \sigma_{ij}\boldsymbol{e}_i \otimes \boldsymbol{e}_j$, where $\{\boldsymbol{e}_i\}$ is the aforementioned local, spherical, orthonormal basis. We specialize their results for an interior region and drop all terms that violate regularity at $r = 0$. By using a dimensionless coordinate $\tilde{r} = r/R$ and after substituting $x = \cos\vartheta$, we find for the displacements:

$$u_r(\tilde{r}, \vartheta) = R \sum_{n=0}^{\infty} \left[-\frac{n\frac{\lambda}{\mu} + n - 2}{2(2n+3)} A_n \tilde{r}^{n+1} + n B_n \tilde{r}^{n-1} \right] P_n(x), \tag{3.3a}$$

$$u_\vartheta(\tilde{r}, \vartheta) = R \sum_{n=1}^{\infty} \left[-\frac{(n+3)\frac{\lambda}{\mu} + n + 5}{2(n+1)(2n+3)} A_n \tilde{r}^{n+1} + B_n \tilde{r}^{n-1} \right] \frac{\mathrm{d}P_n(x)}{\mathrm{d}\vartheta}. \tag{3.3b}$$

The stresses read:

$$\sigma_{rr}(\tilde{r}, \vartheta) = \mu \sum_{n=0}^{\infty} \left[-\frac{(n^2 - n - 3)\frac{\lambda}{\mu} + (n+1)(n-2)}{2n+3} A_n \tilde{r}^n + 2n(n-1) B_n \tilde{r}^{n-2} \right] P_n(x), \tag{3.3c}$$

$$\begin{aligned} \sigma_{\vartheta\vartheta}(\tilde{r}, \vartheta) = {} & \mu \sum_{n=0}^{\infty} \left[\frac{(n+3)\frac{\lambda}{\mu} - n + 2}{2n+3} A_n \tilde{r}^n + 2n B_n \tilde{r}^{n-2} \right] P_n(x) + \\ & + \mu \sum_{n=2}^{\infty} \left[-\frac{(n+3)\frac{\lambda}{\mu} + n + 5}{(n+1)(2n+3)} A_n \tilde{r}^n + 2 B_n \tilde{r}^{n-2} \right] \frac{\mathrm{d}^2 P_n(x)}{\mathrm{d}\vartheta^2}, \end{aligned} \tag{3.3d}$$

$$\sigma_{\varphi\varphi}(\tilde{r},\vartheta) = \mu \sum_{n=0}^{\infty} \left[\frac{(n+3)\frac{\lambda}{\mu} - n + 2}{2n+3} A_n \tilde{r}^n + 2n B_n \tilde{r}^{n-2} \right] P_n(x) + \\ + \mu \sum_{n=1}^{\infty} \left[- \frac{(n+3)\frac{\lambda}{\mu} + n + 5}{(n+1)(2n+3)} A_n \tilde{r}^n + 2 B_n \tilde{r}^{n-2} \right] \frac{\mathrm{d}P_n(x)}{\mathrm{d}\vartheta} \cot(\vartheta), \tag{3.3e}$$

$$\sigma_{r\vartheta}(\tilde{r},\vartheta) = \mu \sum_{n=1}^{\infty} \left[- \frac{n(n+2)\frac{\lambda}{\mu} + n^2 + 2n - 1}{(n+1)(2n+3)} A_n \tilde{r}^n + 2(n-1) B_n \tilde{r}^{n-2} \right] \frac{\mathrm{d}P_n(x)}{\mathrm{d}\vartheta}, \tag{3.3f}$$

$$\sigma_{r\varphi}(\tilde{r},\vartheta) = \sigma_{\vartheta\varphi}(\tilde{r},\vartheta) = 0. \tag{3.3g}$$

The goal is now to find the coefficients A_n and B_n in both problems by exploiting the jump conditions of linear momentum. Since the LORENTZ surface force is contained in these conditions, it has to be specified in order to proceed. This force depends upon the jump of the magnetization and the mean value of the magnetic flux density, which is calculated in the next section.

4 The magnetic field

For the problem of the uniformly magnetized sphere, it is convenient to determine the free current potential, $\mathfrak{H}$, first, instead of the magnetic flux density, $\boldsymbol{B}$. This is a well-known problem covered in many treatises of electrodynamics, e.g., in [4,7,16]. It is commonly used to demonstrate several solution techniques. We briefly review a solution by means of a series expansion, cf., [4], since this method is closely related to the solution of the elastic problem.

The obtained solution of a uniformly magnetized sphere can be modified to the case of a linear magnet under the influence of an uniform exterior field. This is done by employing a neat trick as demonstrated in [7, Sect. 5.11].

4.1 Uniformly magnetized sphere

Due to the curl-free relation $\nabla \times \mathfrak{H} = \mathbf{0}$ both inside and outside the sphere, we may introduce a scalar potential by putting $\mathfrak{H} = -\nabla V_\mathrm{m}$. Since $\nabla \cdot \mathfrak{H} = 0$, we obtain a LAPLACE problem for the potential:

$$\begin{aligned} \Delta V_\mathrm{m} &= 0 && \text{inside and outside the magnet,} \\ \boldsymbol{n} \cdot [\![\nabla V_\mathrm{m}]\!] = \boldsymbol{n} \cdot [\![\boldsymbol{M}_{(\mathrm{I})}]\!], \quad \boldsymbol{n} \times [\![\nabla V_\mathrm{m}]\!] &= \mathbf{0} && \text{between the magnet and the exterior, and} \\ \lim_{\tilde{r}\to\infty} V_\mathrm{m} &= 0 && \text{at infinity.} \end{aligned} \tag{4.1}$$

The general solution of the LAPLACE equation for problems with azimuthal symmetry that is regular at the poles is given by:

$$V_\mathrm{m}(\tilde{r},\vartheta) = \sum_{n=0}^{\infty} \left(C_n \tilde{r}^n + D_n \tilde{r}^{-(n+1)} \right) P_n(x). \tag{4.2}$$

We denote the potentials inside and outside of the magnet by V_m^I and V_m^O, respectively. Regularity of the potential requires that all $C_n = 0$ for the interior solution. Also, since the potential must vanish at infinity, we have $D_n = 0$ in the exterior solution. We may therefore write the potentials as:

$$V_\mathrm{m}^\mathrm{I} = \sum_{n=0}^{\infty} C_n \tilde{r}^n P_n(x), \qquad V_\mathrm{m}^\mathrm{O} = \sum_{n=0}^{\infty} D_n \tilde{r}^{-(n+1)} P_n(x). \tag{4.3}$$

The coefficients C_n and D_n are determined by the jump conditions. The tangential jump condition immediately yields with $\boldsymbol{n} = \boldsymbol{e}_r$:

$$\boldsymbol{e}_r \times [\![\nabla V_\mathrm{m}]\!] = \mathbf{0} \quad \Rightarrow \quad \left.\frac{\mathrm{d}V_\mathrm{m}^\mathrm{I}}{\mathrm{d}\vartheta}\right|_{\tilde{r}=1} = \left.\frac{\mathrm{d}V_\mathrm{m}^\mathrm{O}}{\mathrm{d}\vartheta}\right|_{\tilde{r}=1} \Rightarrow \quad C_n = D_n. \tag{4.4}$$

The right-hand side of the radial jump equation for the potentials is given by:

$$\boldsymbol{e}_r \cdot [\![\boldsymbol{M}_{(\mathrm{I})}]\!] = \boldsymbol{e}_r \cdot (\boldsymbol{0} - M_0 \boldsymbol{e}_z) = -M_0 \cos\vartheta = -M_0 x = -M_0 P_1(x). \tag{4.5}$$

Therefore, the radial jump condition reads:

$$\begin{aligned} &\boldsymbol{e}_r \cdot [\![\nabla V_{\mathrm{m}}]\!] = -M_0 P_1(x) \quad \Leftrightarrow \quad \frac{\mathrm{d}V_{\mathrm{m}}^{\mathrm{O}}}{\mathrm{d}\tilde{r}}\bigg|_{\tilde{r}=1} - \frac{\mathrm{d}V_{\mathrm{m}}^{\mathrm{I}}}{\mathrm{d}\tilde{r}}\bigg|_{\tilde{r}=1} = -RM_0 P_1(x), \quad \text{i.e.,} \\ &\sum_{n=0}^{\infty} C_n (2n+1) P_n(x) = RM_0 P_1(x) \quad \Rightarrow \quad C_1 = \tfrac{1}{3} RM_0, \quad C_n = 0 \,\forall\, n \in \mathbb{N}^0 \backslash \{1\}. \end{aligned} \tag{4.6}$$

Consequently, the scalar potentials are fully determined and the current potential reads:

$$\mathfrak{H}_{(\mathrm{I})}^{\mathrm{I}} = -\frac{M_0}{3}\left(P_1(x)\boldsymbol{e}_r + \frac{\mathrm{d}P_1(x)}{\mathrm{d}\vartheta}\boldsymbol{e}_\vartheta\right) \quad \text{and} \quad \mathfrak{H}_{(\mathrm{I})}^{\mathrm{O}} = -\frac{M_0}{3}\tilde{r}^{-3}\left(-2P_1(x)\boldsymbol{e}_r + \frac{\mathrm{d}P_1(x)}{\mathrm{d}\vartheta}\boldsymbol{e}_\vartheta\right). \tag{4.7}$$

The interior solution is homogeneous, because of the simple relation:

$$P_1(x)\boldsymbol{e}_r + \frac{\mathrm{d}P_1(x)}{\mathrm{d}\vartheta}\boldsymbol{e}_\vartheta = \cos\vartheta \boldsymbol{e}_r - \sin\vartheta \boldsymbol{e}_\vartheta = \boldsymbol{e}_z. \tag{4.8}$$

After using this relation in order to characterize the constant magnetization and by employing the equation $\boldsymbol{B} = \mu_0(\mathfrak{H} + \boldsymbol{M})$, the magnetic flux density reads:

$$\boldsymbol{B}_{(\mathrm{I})}^{\mathrm{I}} = \frac{2}{3}\mu_0 M_0 \left(P_1(x)\boldsymbol{e}_r + \frac{\mathrm{d}P_1(x)}{\mathrm{d}\vartheta}\boldsymbol{e}_\vartheta\right) = \frac{2}{3}\mu_0 M_0 (\cos\vartheta \boldsymbol{e}_r - \sin\vartheta \boldsymbol{e}_\vartheta), \tag{4.9a}$$

$$\boldsymbol{B}_{(\mathrm{I})}^{\mathrm{O}} = \frac{2}{3}\mu_0 M_0 \tilde{r}^{-3}\left(P_1(x)\boldsymbol{e}_r - \frac{1}{2}\frac{\mathrm{d}P_1(x)}{\mathrm{d}\vartheta}\boldsymbol{e}_\vartheta\right) = \frac{2}{3}\mu_0 M_0 \tilde{r}^{-3}(\cos\vartheta \boldsymbol{e}_r + \tfrac{1}{2}\sin\vartheta \boldsymbol{e}_\vartheta). \tag{4.9b}$$

The field characteristics are shown in Fig. 2.

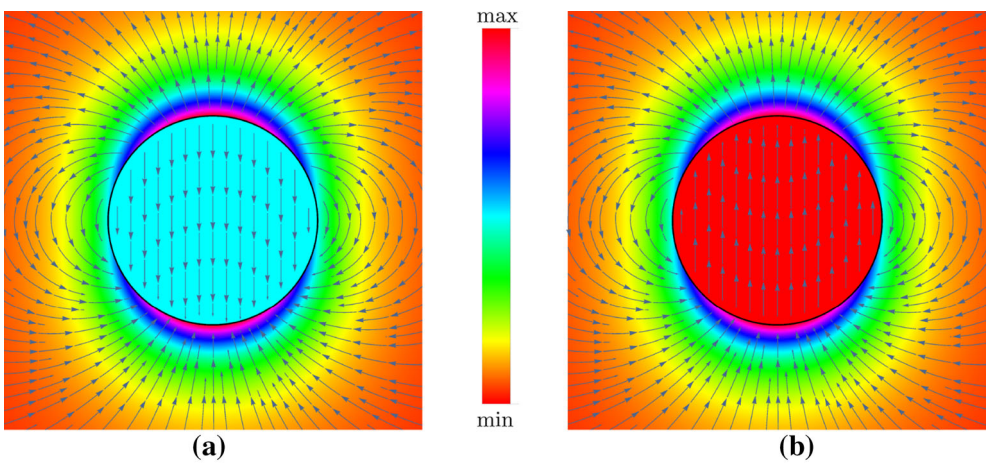

Fig. 2 Streamlines of the fields $\mathfrak{H}_{(\mathrm{I})}$ and $\boldsymbol{B}_{(\mathrm{I})}$ for a uniformly magnetized sphere. *Colors* indicate the norm of the corresponding field. The geometry of the sphere is outlined in *black*. **a** Free current potential $\mathfrak{H}_{(\mathrm{I})}$. **b** Magnetic flux density $\boldsymbol{B}_{(\mathrm{I})}$ (color figure online)

4.2 Linear magnet in an external field

The method outlined in [7, Sect. 5.11] starts by noting that the solution for the magnetic flux density and the free current potential in the interior of the previously analyzed permanent magnet can be written as:

$$\boldsymbol{B}^{\mathrm{I}}_{(\mathrm{I})} = \tfrac{2}{3}\mu_0 \boldsymbol{M}_{(\mathrm{I})}, \quad \boldsymbol{\mathfrak{H}}^{\mathrm{I}}_{(\mathrm{I})} = -\tfrac{1}{3}\boldsymbol{M}_{(\mathrm{I})}, \tag{4.10}$$

where $\boldsymbol{M}^{(\mathrm{I})} = M_0 \boldsymbol{e}_z$. The field equations are linear, consequently, we may superpose the solution by a uniform external field, $\boldsymbol{\mathfrak{H}}^{\mathrm{S}}$, say. The corresponding superposed flux density is $\boldsymbol{B}^{\mathrm{S}} = \mu_0 \boldsymbol{\mathfrak{H}}^{\mathrm{S}}$. In the interior of the magnet, we have:

$$\boldsymbol{B}^{\mathrm{SI}} = \mu_0(\boldsymbol{\mathfrak{H}}^{\mathrm{S}} + \tfrac{2}{3}\boldsymbol{M}_{(\mathrm{I})}), \quad \boldsymbol{\mathfrak{H}}^{\mathrm{SI}} = \boldsymbol{\mathfrak{H}}^{\mathrm{S}} - \tfrac{1}{3}\boldsymbol{M}_{(\mathrm{I})}. \tag{4.11}$$

Now, one *requires* the linear relation $\boldsymbol{B}^{\mathrm{SI}} = \mu_0\mu_{\mathrm{r}}\boldsymbol{\mathfrak{H}}^{\mathrm{SI}}$ to hold and *determines* $\boldsymbol{M}_{(\mathrm{II})}$ with a given relative permeability μ_{r}:

$$\mu_0(\boldsymbol{\mathfrak{H}}^{\mathrm{S}} + \tfrac{2}{3}\boldsymbol{M}_{(\mathrm{II})}) = \mu_0\mu_{\mathrm{r}}(\boldsymbol{\mathfrak{H}}^{\mathrm{S}} - \tfrac{1}{3}\boldsymbol{M}_{(\mathrm{II})}) \quad \Leftrightarrow \quad \boldsymbol{M}_{(\mathrm{II})} = 3\frac{\mu_{\mathrm{r}} - 1}{2 + \mu_{\mathrm{r}}}\boldsymbol{\mathfrak{H}}^{\mathrm{S}}. \tag{4.12}$$

By choosing $\boldsymbol{\mathfrak{H}}^{\mathrm{S}} = \mathfrak{H}_0 \boldsymbol{e}_z$ we find for the modified solution:

$$M_0 = 3\frac{\mu_{\mathrm{r}} - 1}{2 + \mu_{\mathrm{r}}}\mathfrak{H}_0. \tag{4.13}$$

And therefore the relevant superposed fields of the linear-magnetic sphere become:

$$\boldsymbol{B}^{\mathrm{SI}}_{(\mathrm{II})} = \mu_0\mathfrak{H}_0\frac{3\mu_{\mathrm{r}}}{2 + \mu_{\mathrm{r}}}(\cos\vartheta\,\boldsymbol{e}_r - \sin\vartheta\,\boldsymbol{e}_\vartheta), \tag{4.14a}$$

$$\boldsymbol{B}^{\mathrm{SO}}_{(\mathrm{II})} = \mu_0\mathfrak{H}_0\left(\left[1 + 2\frac{\mu_{\mathrm{r}} - 1}{2 + \mu_{\mathrm{r}}}\tilde{r}^{-3}\right]\cos\vartheta\,\boldsymbol{e}_r - \left[1 + \frac{1 - \mu_{\mathrm{r}}}{2 + \mu_{\mathrm{r}}}\tilde{r}^{-3}\right]\sin\vartheta\,\boldsymbol{e}_\vartheta\right), \tag{4.14b}$$

and

$$\boldsymbol{\mathfrak{H}}^{\mathrm{SI}}_{(\mathrm{II})} = \mathfrak{H}_0\frac{3}{2 + \mu_{\mathrm{r}}}(\cos\vartheta\,\boldsymbol{e}_r - \sin\vartheta\,\boldsymbol{e}_\vartheta), \tag{4.14c}$$

$$\boldsymbol{\mathfrak{H}}^{\mathrm{SO}}_{(\mathrm{II})} = \mathfrak{H}_0\left(\left[1 + 2\frac{\mu_{\mathrm{r}} - 1}{2 + \mu_{\mathrm{r}}}\tilde{r}^{-3}\right]\cos\vartheta\,\boldsymbol{e}_r - \left[1 + \frac{1 - \mu_{\mathrm{r}}}{2 + \mu_{\mathrm{r}}}\tilde{r}^{-3}\right]\sin\vartheta\,\boldsymbol{e}_\vartheta\right). \tag{4.14d}$$

In what follows we define for practical reasons $\boldsymbol{B}^{\mathrm{I}}_{(\mathrm{II})} := \boldsymbol{B}^{\mathrm{SI}}_{(\mathrm{II})}$, $\boldsymbol{B}^{\mathrm{O}}_{(\mathrm{II})} := \boldsymbol{B}^{\mathrm{SO}}_{(\mathrm{II})}$, $\boldsymbol{\mathfrak{H}}^{\mathrm{I}}_{(\mathrm{II})} := \boldsymbol{\mathfrak{H}}^{\mathrm{SI}}_{(\mathrm{II})}$, and $\boldsymbol{\mathfrak{H}}^{\mathrm{O}}_{(\mathrm{II})} := \boldsymbol{\mathfrak{H}}^{\mathrm{SO}}_{(\mathrm{II})}$. These fields are visualized in Fig. 3.

5 Lorentz surface force density and suitable series expansions

By means of the previously determined magnetic flux densities (4.9) and (4.14) we may now examine surface forces of the form:

$$\boldsymbol{f}^{\mathrm{L}}_{I} = (\boldsymbol{n} \times [\![\boldsymbol{M}]\!]) \times \langle \boldsymbol{B} \rangle$$

for both problems. We start by calculating the mean value of the magnetic flux density in both cases at the sphere's surface. Then we proceed by determining the tangential jump of the individual magnetizations. The force densities follow, and the components are expanded in such a manner that an algebraic system is directly generated from the jump equation of linear momentum. Then the unknown coefficients of the elastic solution can be determined easily.

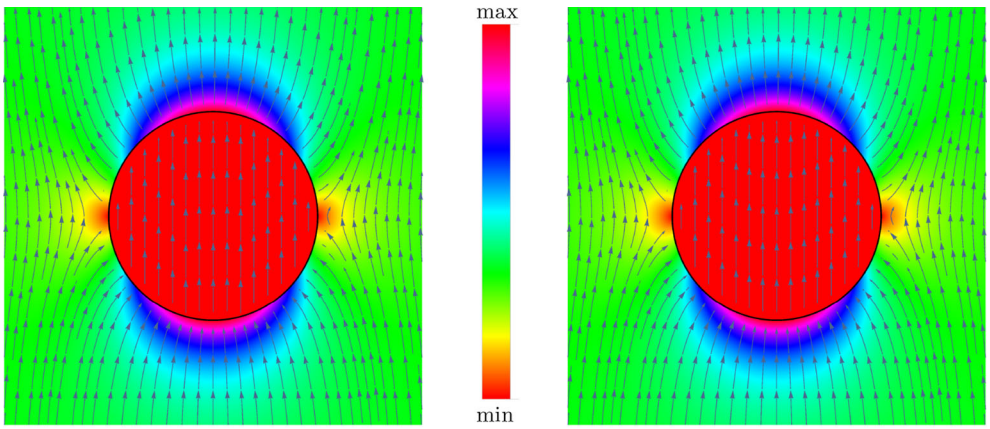

Fig. 3 Streamlines of the fields $\mathfrak{H}_{(\mathrm{II})}$ and $\boldsymbol{B}_{(\mathrm{II})}$ for a linear-magnetic sphere. $\mu_\mathrm{r} = 100$ (steel) was used for visualization. *Colors* indicate the norm of the corresponding field. The geometry of the sphere is outlined in *black*. **a** Free current potential $\mathfrak{H}_{(\mathrm{II})}$. **b** Magnetic flux density $\boldsymbol{B}_{(\mathrm{II})}$ (color figure online)

5.1 Mean value of the magnetic flux

The mean value of the magnetic flux on the surface of the uniformly magnetized sphere is calculated as:

$$\left\langle \boldsymbol{B}_{(\mathrm{I})} \right\rangle = \tfrac{1}{2}(\boldsymbol{B}^{\mathrm{I}}_{(\mathrm{I})} + \boldsymbol{B}^{\mathrm{O}}_{(\mathrm{I})})|_{\tilde{r}=1} = \tfrac{1}{6}\mu_0 M_0 (4\cos\vartheta \boldsymbol{e}_r - \sin\vartheta \boldsymbol{e}_\vartheta). \tag{5.1}$$

For the linear magnet the mean value of the total field reads:

$$\left\langle \boldsymbol{B}_{(\mathrm{II})} \right\rangle = \tfrac{1}{2}(\boldsymbol{B}^{\mathrm{SI}}_{(\mathrm{I})} + \boldsymbol{B}^{\mathrm{SO}}_{(\mathrm{I})})|_{\tilde{r}=1} = \frac{3}{2}\frac{\mu_0 \mathfrak{H}_0}{2+\mu_\mathrm{r}} \left[2\mu_\mathrm{r}\cos\vartheta \boldsymbol{e}_r - (1+\mu_\mathrm{r})\sin\vartheta \boldsymbol{e}_\vartheta\right]. \tag{5.2}$$

5.2 Tangential jump of magnetization

By using $\boldsymbol{n} = \boldsymbol{e}_r$ the vector product can be evaluated and we obtain for the uniformly magnetized sphere:

$$\boldsymbol{n} \times [\![\boldsymbol{M}_{(\mathrm{I})}]\!] = -M_0 \boldsymbol{e}_r \times \boldsymbol{e}_z = -M_0 \boldsymbol{e}_r \times (\cos\vartheta \boldsymbol{e}_r - \sin\vartheta \boldsymbol{e}_\vartheta) = M_0 \sin\vartheta \boldsymbol{e}_\varphi. \tag{5.3}$$

This also directly applies to the linear magnet, because in that case $M_0 = 3^{(\mu_\mathrm{r}-1)/(2+\mu_\mathrm{r})}\mathfrak{H}_0$. Hence:

$$\boldsymbol{n} \times [\![\boldsymbol{M}_{(\mathrm{II})}]\!] = 3\mathfrak{H}_0 \frac{\mu_\mathrm{r}-1}{2+\mu_\mathrm{r}} \sin\vartheta \boldsymbol{e}_\varphi. \tag{5.4}$$

5.3 Force densities

We compute the force in both cases:

$$\begin{aligned} \boldsymbol{f}^{\mathrm{L}}_{I\,(\mathrm{I})} &= (\boldsymbol{n} \times [\![\boldsymbol{M}_{(\mathrm{I})}]\!]) \times \left\langle \boldsymbol{B}_{(\mathrm{I})} \right\rangle = \tfrac{1}{6}\mu_0 M_0^2 (\sin^2\vartheta \boldsymbol{e}_r + 4\sin\vartheta\cos\vartheta \boldsymbol{e}_\vartheta), \\ \boldsymbol{f}^{\mathrm{L}}_{I\,(\mathrm{II})} &= (\boldsymbol{n} \times [\![\boldsymbol{M}_{(\mathrm{II})}]\!]) \times \left\langle \boldsymbol{B}_{(\mathrm{II})} \right\rangle = \tfrac{9}{2}\mu_0 \mathfrak{H}_0^2 \frac{\mu_\mathrm{r}-1}{(2+\mu_\mathrm{r})^2} [(1+\mu_\mathrm{r})\sin^2\vartheta \boldsymbol{e}_r + 2\mu_\mathrm{r}\sin\vartheta\cos\vartheta \boldsymbol{e}_\vartheta]. \end{aligned} \tag{5.5}$$

Note that the radial and polar components of both force densities merely differ by a constant factor. The components show the same dependence on the polar angle, see Fig. 4. However, the resulting vectors differ significantly in direction and magnitude, cf., Fig. 5. Due to their same angular dependencies, we can examine both problems simultaneously by defining:

$$\hat{\sigma}^{(\mathrm{I})} = \mu_0 M_0^2, \quad a^{(\mathrm{I})} = \tfrac{1}{6}, \quad b^{(\mathrm{I})} = \tfrac{2}{3}, \quad \hat{\sigma}^{(\mathrm{II})} = \mu_0 \mathfrak{H}_0^2, \quad a^{(\mathrm{II})} = \tfrac{9}{2}\frac{(\mu_\mathrm{r}-1)(1+\mu_\mathrm{r})}{(2+\mu_\mathrm{r})^2}, \quad b^{(\mathrm{II})} = 9\frac{\mu_\mathrm{r}(\mu_\mathrm{r}-1)}{(2+\mu_\mathrm{r})^2} \tag{5.6}$$

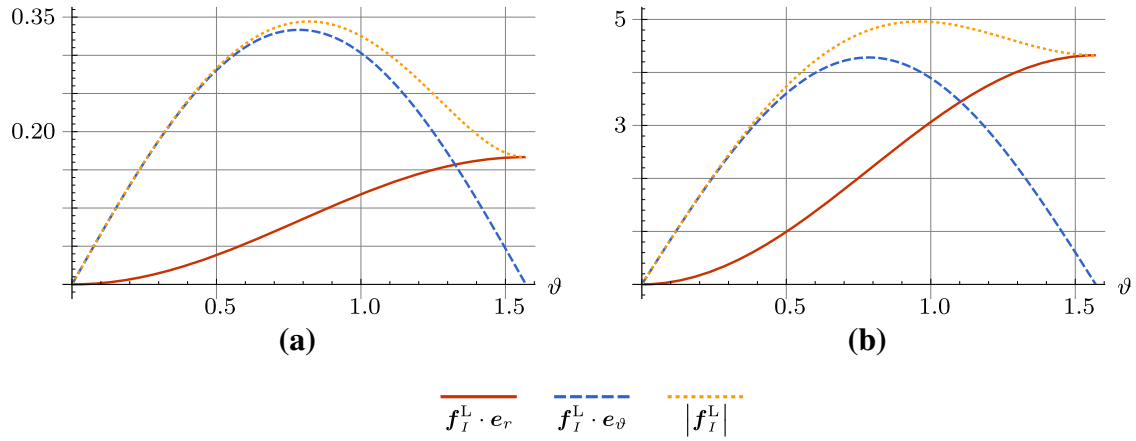

Fig. 4 Components and magnitudes of the LORENTZ surface traction for both problems plotted against the polar angle $\vartheta \in [0, \pi/2]$. In **b**, $\mu_{\mathrm{r}} = 100$ was used for visualization. **a** Uniformly magnetized sphere, all values normalized by $\hat{\sigma}^{(\mathrm{I})}$. **b** Linear-magnetic sphere in an external field, all values normalized by $\hat{\sigma}^{(\mathrm{II})}$

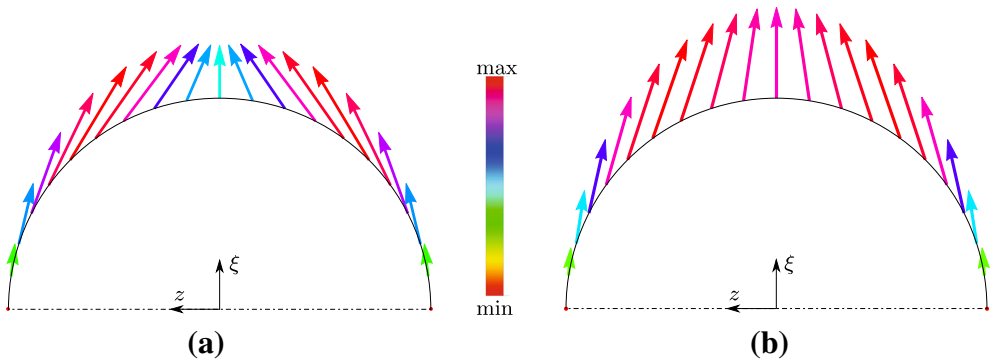

Fig. 5 Qualitative representations of the LORENTZ surface traction for both problems in a half-plane of symmetry. Note that different scaling factors were applied. In **b**, $\mu_{\mathrm{r}} = 100$ was used. For visualization purposes cylindrical coordinates (ξ, z) were used for a constant azimuthal angle. **a** Uniformly magentized sphere. **b** Linear-magnetic sphere in external field

with the functions:

$$f_r(\vartheta) = \sin^2\vartheta = 1 - x^2, \quad f_\vartheta(\vartheta) = \sin\vartheta\cos\vartheta = x\sqrt{1-x^2}. \tag{5.7}$$

Thus, we denote compactly:

$$\boldsymbol{f}^{\mathrm{L}}_{I\,(\mathrm{I})} = \hat{\sigma}^{(\mathrm{I})}(a^{(\mathrm{I})} f_r(\vartheta)\boldsymbol{e}_r + b^{(\mathrm{I})} f_\vartheta(\vartheta)\boldsymbol{e}_\vartheta), \quad \boldsymbol{f}^{\mathrm{L}}_{I\,(\mathrm{II})} = \hat{\sigma}^{(\mathrm{II})}(a^{(\mathrm{II})} f_r(\vartheta)\boldsymbol{e}_r + b^{(\mathrm{II})} f_\vartheta(\vartheta)\boldsymbol{e}_\vartheta). \tag{5.8}$$

The angular functions in the components of the force, f_r and f_ϑ are now expanded in a suitable manner in order to solve the elastic problem successively.

5.4 The radial function

The dependence of the radial stress σ_{rr} on the polar angle is solely given in terms of LEGENDRE polynomials, see Eq. (3.3c). The radial component of the LORENTZ force density is directly connected to the radial stress by the jump condition of linear momentum. In order to derive an algebraic system, we choose to expand the function $f_r(\vartheta)$ in LEGENDRE polynomials, namely:

$$f_r(\vartheta) = 1 - x^2 = \sum_{n=0}^{\infty} c_n P_n. \tag{5.9}$$

We note the formulae:

$$P_0(x) = 1, \quad P_2(x) = \tfrac{1}{2}(3x^2 - 1) \quad \Leftrightarrow \quad x^2 = \tfrac{1}{3}P_0(x) + \tfrac{2}{3}P_2(x) \tag{5.10}$$

and write directly:

$$1 - x^2 = \tfrac{2}{3} P_0(x) - \tfrac{2}{3} P_2(x) \quad \Rightarrow \quad c_0 = \tfrac{2}{3}, \quad c_2 = -\tfrac{2}{3}, \quad c_n = 0 \,\forall\, n \in \mathbb{N}^0 \backslash \{0, 2\}. \tag{5.11}$$

5.5 The polar function

The dependence of the shear stress $\sigma_{r\vartheta}$ on the polar angle is exclusively given by derivatives of LEGENDRE polynomials, cf., Eq. (3.3f). Due to the mathematical structure of the tangential jump equation of linear momentum, we expand the polar function $f_\vartheta(\vartheta)$ in the form:

$$f_\vartheta(\vartheta) = x\sqrt{1 - x^2} = \sum_{n=1}^{\infty} k_n \frac{\mathrm{d}P_n}{\mathrm{d}\vartheta}. \tag{5.12}$$

We start by representing x with:

$$\frac{\mathrm{d}P_2}{\mathrm{d}x} = \frac{1}{2}\frac{\mathrm{d}}{\mathrm{d}x}(3x^2 - 1) = 3x \quad \Leftrightarrow \quad x = \frac{1}{3}\frac{\mathrm{d}P_2}{\mathrm{d}x} = -\frac{1}{3}\frac{1}{\sqrt{1 - x^2}}\frac{\mathrm{d}P_2}{\mathrm{d}\vartheta}. \tag{5.13}$$

When using this relation the polar function follows:

$$f_\vartheta(\vartheta) = -\frac{1}{3}\frac{\mathrm{d}P_2}{\mathrm{d}\vartheta} \quad \Leftrightarrow \quad k_2 = -\tfrac{1}{3}, \quad k_n = 0 \,\forall\, n \in \mathbb{N}^0 \backslash \{0, 2\}. \tag{5.14}$$

Note that k_0 is not contained in the series and therefore arbitrary.

6 Solution of the elastic problem

By virtue of the previously expanded generalized surface force densities for both problems, the jump equation of linear momentum can be evaluated and yields algebraic equations for the unknown coefficients of the displacement field, A_n and B_n. We recall that stresses outside the magnet are neglected and that $\sigma_{r\varphi}$ is zero inside the magnet due to the semi-inverse *ansatz*. Using that the jump equation reads:

$$\boldsymbol{n} \cdot [\![\boldsymbol{\sigma}_{(\mathrm{I/II})}]\!] = -\boldsymbol{f}^{\mathrm{L}}_{I\,(\mathrm{I/II})} \quad \text{with} \quad \boldsymbol{n} \cdot [\![\boldsymbol{\sigma}_{(\mathrm{I/II})}]\!] = -\boldsymbol{e}_r \cdot \boldsymbol{\sigma}_{(\mathrm{I/II})}(\tilde{r} = 1, \vartheta) \tag{6.1}$$

yields after projection onto $\boldsymbol{e}_r$ and $\boldsymbol{e}_\vartheta$:

$$\begin{aligned} \boldsymbol{e}_r \cdot \boldsymbol{\sigma}_{(\mathrm{I/II})}(\tilde{r} = 1, \vartheta) \cdot \boldsymbol{e}_r = \boldsymbol{f}^{\mathrm{L}}_{I\,(\mathrm{I/II})}(\vartheta) \cdot \boldsymbol{e}_r \quad &\Leftrightarrow \quad \sigma^{(\mathrm{I/II})}_{rr}(\tilde{r} = 1, \vartheta) = \hat{\sigma}^{(\mathrm{I/II})} a^{(\mathrm{I/II})} f_r(\vartheta), \\ \boldsymbol{e}_r \cdot \boldsymbol{\sigma}_{(\mathrm{I/II})}(\tilde{r} = 1, \vartheta) \cdot \boldsymbol{e}_\vartheta = \boldsymbol{f}^{\mathrm{L}}_{I\,(\mathrm{I/II})}(\vartheta) \cdot \boldsymbol{e}_\vartheta \quad &\Leftrightarrow \quad \sigma^{(\mathrm{I/II})}_{r\vartheta}(\tilde{r} = 1, \vartheta) = \hat{\sigma}^{(\mathrm{I/II})} b^{(\mathrm{I/II})} f_\vartheta(\vartheta). \end{aligned} \tag{6.2}$$

These two relations read explicitly:

$$\begin{aligned} \mu \sum_{n=0}^{\infty} \Bigg[&- \frac{(n^2 - n - 3)\frac{\lambda}{\mu} + (n+1)(n-2)}{2n+3} A_n^{(\mathrm{I/II})} + \\ &+ 2n(n-1) B_n^{(\mathrm{I/II})} \Bigg] P_n(x) = \tfrac{2}{3}\hat{\sigma}^{(\mathrm{I/II})} a^{(\mathrm{I/II})} P_0(x) - \tfrac{2}{3}\hat{\sigma}^{(\mathrm{I/II})} a^{(\mathrm{I/II})} P_2(x), \end{aligned} \tag{6.3}$$

and

$$\mu \sum_{n=1}^{\infty} \left[- \frac{n(n+2)\frac{\lambda}{\mu} + n^2 + 2n - 1}{(n+1)(2n+3)} A_n^{(\mathrm{I/II})} + 2(n-1) B_n^{(\mathrm{I/II})} \right] \frac{\mathrm{d}P_n(x)}{\mathrm{d}\vartheta} = -\frac{1}{3}\hat{\sigma}^{(\mathrm{I/II})} b^{(\mathrm{I/II})} \frac{\mathrm{d}P_2}{\mathrm{d}\vartheta}. \tag{6.4}$$

Since two polynomials of the same rank are equal if and only if their coefficients are equal, we read off the following relations:

$$\tfrac{2}{3}\hat{\sigma}^{(\mathrm{I/II})} a^{(\mathrm{I/II})} = \mu(\tfrac{\lambda}{\mu} + \tfrac{2}{3}) A_0^{(\mathrm{I/II})}, \tag{6.5a}$$

$$-\tfrac{2}{3}\hat{\sigma}^{(\mathrm{I/II})} a^{(\mathrm{I/II})} = \mu \tfrac{1}{7}\tfrac{\lambda}{\mu} A_2^{(\mathrm{I/II})} + 4\mu B_2^{(\mathrm{I/II})}, \tag{6.5b}$$

and for $n \in \mathbb{N}^0 \backslash \{0, 2\}$:

$$0 = -[(n^2 - n - 3)\tfrac{\lambda}{\mu} + (n+1)(n-2)]A_n^{(\mathrm{I/II})} + 2n(n-1)(2n+3)B_n^{(\mathrm{I/II})}, \tag{6.5c}$$

$$-\tfrac{1}{3}\hat{\sigma}^{(\mathrm{I/II})} b^{(\mathrm{I/II})} = -\mu(\tfrac{8}{21}\tfrac{\lambda}{\mu} + \tfrac{1}{3})A_2^{(\mathrm{I/II})} + 2\mu B_2^{(\mathrm{I/II})}, \tag{6.5d}$$

$$0 = -[n(n+2)\tfrac{\lambda}{\mu} + n^2 + 2n - 1]A_n^{(\mathrm{I/II})} + 2(n-1)(n+1)(2n+3)B_n^{(\mathrm{I/II})}. \tag{6.5e}$$

Alternatively, one could employ the relations of orthogonality shown in Appendix D to find these equations. The solution of this generalized algebraic system is:

$$A_0^{(\mathrm{I/II})} = \frac{\hat{\sigma}^{(\mathrm{I/II})}}{\mu}\frac{2a^{(\mathrm{I/II})}}{3\frac{\lambda}{\mu}+2}, \quad A_2^{(\mathrm{I/II})} = \frac{\hat{\sigma}^{(\mathrm{I/II})}}{\mu}\frac{b^{(\mathrm{I/II})} - a^{(\mathrm{I/II})}}{1+\frac{19}{14}\frac{\lambda}{\mu}}, \quad B_2^{(\mathrm{I/II})} = -\frac{\hat{\sigma}^{(\mathrm{I/II})}}{\mu}\frac{2(8\frac{\lambda}{\mu}+7)a^{(\mathrm{I/II})} + 3\frac{\lambda}{\mu}b^{(\mathrm{I/II})}}{6(19\frac{\lambda}{\mu}+14)}. \tag{6.6}$$

All other coefficients vanish, the problem is solved, and the series in Eq. (3.3) turn into finite sums.

The sphere's displacements in both problems are given by:

$$u_r^{(\mathrm{I/II})}(\tilde{r}, \vartheta) = R\frac{\hat{\sigma}^{(\mathrm{I/II})}}{\mu}\left[\tfrac{1}{3}\hat{A}_0^{(\mathrm{I/II})} + \left(2\hat{B}_2^{(\mathrm{I/II})} - \tfrac{1}{7}\hat{A}_2^{(\mathrm{I/II})}\tfrac{\lambda}{\mu}\tilde{r}^2\right)P_2(x)\right]\tilde{r}, \tag{6.7a}$$

$$u_\vartheta^{(\mathrm{I/II})}(\tilde{r}, \vartheta) = R\frac{\hat{\sigma}^{(\mathrm{I/II})}}{\mu}\left[\hat{B}_2^{(\mathrm{I/II})} - \tfrac{1}{42}\hat{A}_2^{(\mathrm{I/II})}(5\tfrac{\lambda}{\mu}+7)\tilde{r}^2\right]\tilde{r}\frac{\mathrm{d}P_2(x)}{\mathrm{d}\vartheta}, \tag{6.7b}$$

and due to symmetry we have $u_\varphi^{(\mathrm{I/II})}(\tilde{r}, \vartheta) = 0$. The stresses follow as:

$$\sigma_{rr}^{(\mathrm{I/II})}(\tilde{r}, \vartheta) = \hat{\sigma}^{(\mathrm{I/II})}\left[\tfrac{1}{3}(2+3\tfrac{\lambda}{\mu})\hat{A}_0^{(\mathrm{I/II})} + \left(4\hat{B}_2^{(\mathrm{I/II})} + \tfrac{1}{7}\tfrac{\lambda}{\mu}\hat{A}_2^{(\mathrm{I/II})}\tilde{r}^2\right)P_2(x)\right], \tag{6.8a}$$

$$\sigma_{\vartheta\vartheta}^{(\mathrm{I/II})}(\tilde{r}, \vartheta) = \hat{\sigma}^{(\mathrm{I/II})}\left[\left(\tfrac{2}{3}+\tfrac{\lambda}{\mu}\right)\hat{A}_0^{(\mathrm{I/II})} + \left(4\hat{B}_2^{(\mathrm{I/II})} + \tfrac{5}{7}\tfrac{\lambda}{\mu}\hat{A}_2^{(\mathrm{I/II})}\tilde{r}^2\right)P_2(x) + \right.$$
$$\left. + \left(2\hat{B}_2^{(\mathrm{I/II})} - (\tfrac{1}{3}+\tfrac{5}{21}\tfrac{\lambda}{\mu})\hat{A}_2^{(\mathrm{I/II})}\tilde{r}^2\right)\frac{\mathrm{d}^2P_2(x)}{\mathrm{d}\vartheta^2}\right], \tag{6.8b}$$

$$\sigma_{\varphi\varphi}^{(\mathrm{I/II})}(\tilde{r}, \vartheta) = \hat{\sigma}^{(\mathrm{I/II})}\left[\left(\tfrac{2}{3}+\tfrac{\lambda}{\mu}\right)\hat{A}_0^{(\mathrm{I/II})} + \left(4\hat{B}_2^{(\mathrm{I/II})} + \tfrac{5}{7}\tfrac{\lambda}{\mu}\hat{A}_2^{(\mathrm{I/II})}\tilde{r}^2\right)P_2(x) + \right.$$
$$\left. + \left(2\hat{B}_2^{(\mathrm{I/II})} - (\tfrac{1}{3}+\tfrac{5}{21}\tfrac{\lambda}{\mu})\hat{A}_2^{(\mathrm{I/II})}\tilde{r}^2\right)\cot\vartheta\frac{\mathrm{d}P_2(x)}{\mathrm{d}\vartheta}\right], \tag{6.8c}$$

$$\sigma_{r\vartheta}^{(\mathrm{I/II})}(\tilde{r}, \vartheta) = \hat{\sigma}^{(\mathrm{I/II})}\left[2\hat{B}_2^{(\mathrm{I/II})} - (\tfrac{1}{3}+\tfrac{8}{21}\tfrac{\lambda}{\mu})\hat{A}_2^{(\mathrm{I/II})}\tilde{r}^2\right]\frac{\mathrm{d}P_2(x)}{\mathrm{d}\vartheta}, \tag{6.8d}$$

and the shear stresses $\sigma_{r\varphi}^{(\mathrm{I/II})}(\tilde{r}, \vartheta)$ and $\sigma_{\vartheta\varphi}^{(\mathrm{I/II})}(\tilde{r}, \vartheta)$ vanish. The enclosed functions related to LEGENDRE polynomials are:

$$P_2(x) = \tfrac{3}{2}\cos^2\vartheta - \tfrac{1}{2}, \quad \frac{\mathrm{d}P_2(x)}{\mathrm{d}\vartheta} = -3\sin\vartheta\cos\vartheta \quad \text{and} \quad \frac{\mathrm{d}^2P_2(x)}{\mathrm{d}\vartheta^2} = 3\sin^2\vartheta - 3\cos^2\vartheta.$$

The employed constants are in case of a *uniformly magnetized sphere*:

$$\hat{\sigma}^{(\mathrm{I})} = \mu_0 M_0^2, \quad \hat{A}_0^{(\mathrm{I})} = \frac{1}{6+9\frac{\lambda}{\mu}}, \quad \hat{A}_2^{(\mathrm{I})} = \frac{7}{14+19\frac{\lambda}{\mu}}, \quad \hat{B}_2^{(\mathrm{I})} = -\frac{7(1+2\frac{\lambda}{\mu})}{252+342\frac{\lambda}{\mu}}. \tag{6.9}$$

For the *linear-magnetic sphere* under the influence of an external field of magnitude $\mathfrak{H}_0$, the resulting constants are

$$\hat{\sigma}^{(\mathrm{II})} = \mu_0\mathfrak{H}_0^2, \qquad \hat{A}_0^{(\mathrm{II})} = \frac{9(\mu_\mathrm{r}^2-1)}{(2+3\frac{\lambda}{\mu})(2+\mu_\mathrm{r})^2},$$

$$\hat{A}_2^{(\mathrm{II})} = \frac{63(\mu_\mathrm{r}-1)^2}{(14+19\frac{\lambda}{\mu})(2+\mu_\mathrm{r})^2}, \qquad \hat{B}_2^{(\mathrm{II})} = -\frac{3(\mu_\mathrm{r}-1)(7+8\frac{\lambda}{\mu}+(7+11\frac{\lambda}{\mu})\mu_\mathrm{r})}{2(14+19\frac{\lambda}{\mu})(2+\mu_\mathrm{r})^2}. \tag{6.10}$$

7 Analysis of the results

We start the section with a brief analysis of limiting cases for the LORENTZ traction of the linear magnet w.r.t. the relative permeability μ_r. Then we proceed to examine the solutions of the elastic problems: Displacements, strains, and stresses of both spherical problems will be evaluated and discussed.

7.1 Paramagnetic and diamagnetic force limits

Depending on μ_r the amplifying function for the linear magnet can be significantly higher in magnitude than the corresponding functions of the permanent magnet. In what follows we will refer to media with $\mu_\mathrm{r} < 1$ as *diamagetic* and those with $\mu_\mathrm{r} > 1$ as *paramagnetic*. It is interesting to note that the change of force in the linear magnet due to change of relative permeability μ_r is limited. This can be seen by examining the relevant factors of the force components $a^{(\mathrm{II})}$ and $b^{(\mathrm{II})}$ in Eq. (5.8):

$$\begin{aligned}
\lim_{\mu_\mathrm{r}\to\infty} a^{(\mathrm{II})} &= \lim_{\mu_\mathrm{r}\to\infty} \frac{9}{2}\frac{(\mu_\mathrm{r}-1)(1+\mu_\mathrm{r})}{(2+\mu_\mathrm{r})^2} = \frac{9}{2}, \quad \lim_{\mu_\mathrm{r}\to\infty} b^{(\mathrm{II})} = \lim_{\mu_\mathrm{r}\to\infty} 9\frac{\mu_\mathrm{r}(\mu_\mathrm{r}-1)}{(2+\mu_\mathrm{r})^2} = 9\,, \quad \text{and} \\
\lim_{\mu_\mathrm{r}\searrow 0} a^{(\mathrm{II})} &= \lim_{\mu_\mathrm{r}\searrow 0} \frac{9}{2}\frac{(\mu_\mathrm{r}-1)(1+\mu_\mathrm{r})}{(2+\mu_\mathrm{r})^2} = -\frac{9}{8}\,, \quad \lim_{\mu_\mathrm{r}\searrow 0} b^{(\mathrm{II})} = \lim_{\mu_\mathrm{r}\searrow 0} 9\frac{\mu_\mathrm{r}(\mu_\mathrm{r}-1)}{(2+\mu_\mathrm{r})^2} = 0.
\end{aligned} \tag{7.1}$$

Hence, the force limits of the linear magnet w.r.t. the relative permeability are explicitly given by:

$$\lim_{\mu_\mathrm{r}\to\infty} \boldsymbol{f}^{\mathrm{L}}_{I\,(\mathrm{II})} = \frac{9}{2}\mu_0\mathfrak{H}_0^2 \sin\vartheta\,(\sin\vartheta\,\boldsymbol{e}_r + 2\cos\vartheta\,\boldsymbol{e}_\vartheta)\,, \qquad \text{(paramagentic force limit)} \tag{7.2a}$$

$$\lim_{\mu_\mathrm{r}\searrow 0} \boldsymbol{f}^{\mathrm{L}}_{I\,(\mathrm{II})} = -\frac{9}{2}\mu_0\mathfrak{H}_0^2 \sin^2\vartheta\,\boldsymbol{e}_r. \qquad \text{(diamagnetic force limit)} \tag{7.2b}$$

Thus, with the LORENTZ force model a purely normal traction can only be obtained in the diamagnetic force limit. For the permanent magnet, a purely normal traction is impossible.

7.2 Displacements

The dimension and scale of the displacements are primarily governed by the factors $R\hat{\sigma}^{(\mathrm{I/II})}\mu^{-1}$. Therefore, the normalization $u_i^{(\mathrm{I/II})} = R\hat{\sigma}^{(\mathrm{I/II})}\mu^{-1}\tilde{u}_i^{(\mathrm{I/II})}$ is employed. By considering Fig. 6 it can be seen that the displacements at the poles and the equator are purely radial in both problems—this property is independent of the problems' physical parameters. Note that for a fixed $\tilde{r}$, the largest displacements neither occur at the poles nor at the equator. This can clearly be observed in Fig. 6c, d. The angle of largest displacement for a given $\tilde{r}$ depends upon the material parameters λ/μ and μ_r.

Furthermore, the equatorial plane is a plane of symmetry for the displacement field in both magnetic problems. For this reason, the components of displacement in Fig. 6 are only visualized in the region $\vartheta \in [0, \pi/2]$. In the remanent magnetic problem, the polar displacement is always positive. The same holds for the linear magnet, provided that the considered medium is paramagnetic. There is always a change of sign in the radial displacement of both problems—this is clearly visible in the figures with variation of the polar angle, see Fig. 6e, f.

Note that all displacements in Eq. (6.7) are linear in the sphere's initial radius R. However, the magnitude of the problems' displacements is primarily governed by the factors $\hat{\sigma}^{(\mathrm{I/II})}/\mu$. For example, consider a permanent magnet with a remanence of about one tesla and steel-like elastic behavior. Here, the factor is of the order 10^{-5}. In the linear-magnetic sphere, this ratio can be increased by enlarging the external field within the linear region of the virgin magnetization curve. Hence this increase is limited. In practice, it is therefore difficult to measure displacements of magnets with small spatial extension.

7.3 Strains

First, the strain tensor $\boldsymbol{\varepsilon}$ is formed according to Eq. $(2.9)_2$. Due to the structure of the displacement field, the component matrix of this tensor w.r.t. the orthonormal spherical basis possesses off-diagonal entries. Therefore,

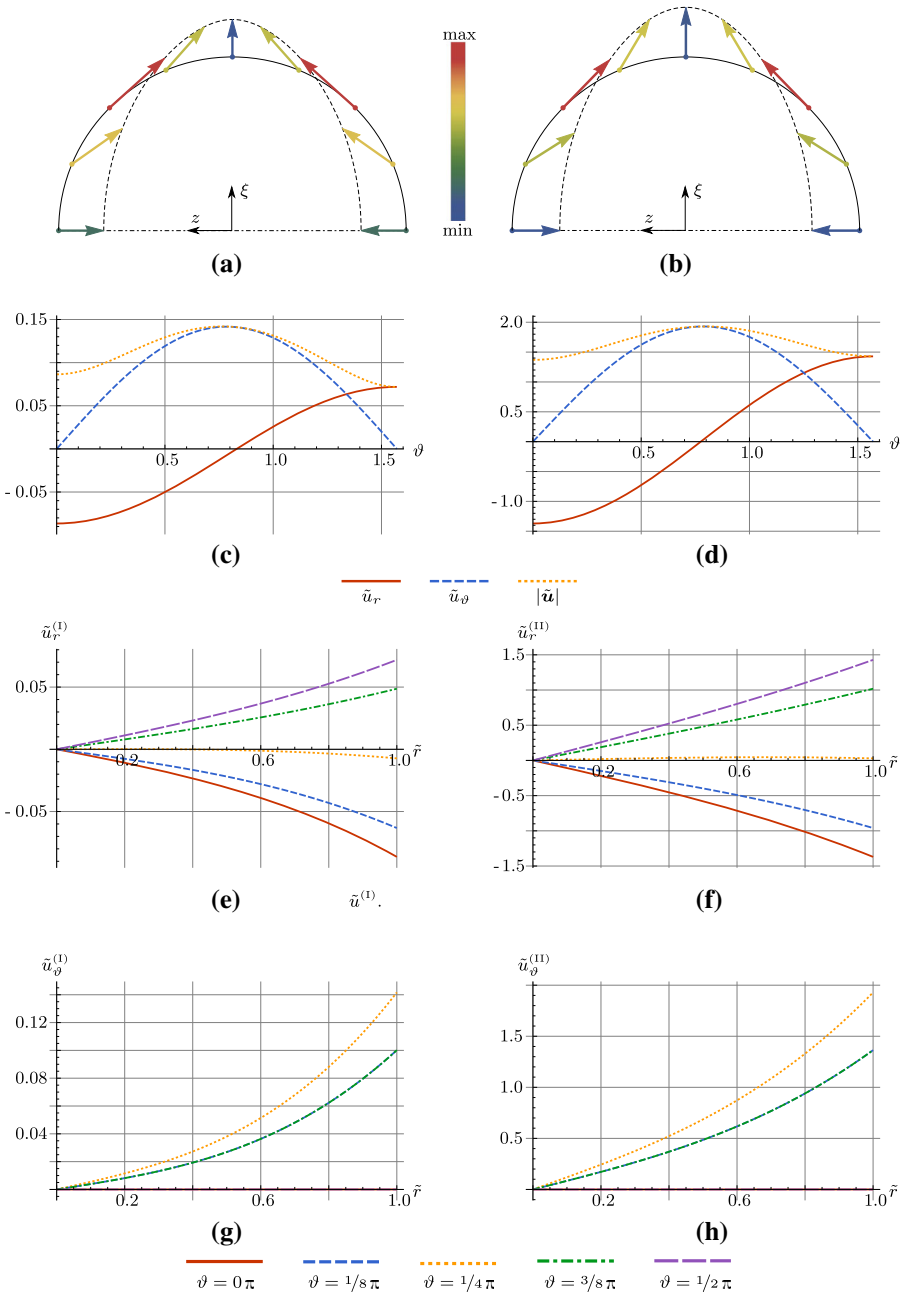

Fig. 6 Displacements for both the permanent magnetic sphere and the linear-magnetic sphere in an external field. The ratio $\lambda/\mu = 1.27$ was used for both cases and $\mu_\mathrm{r} = 100$ for the linear magnet. In **a**, **b**, the normalized displacement vectors on the surface are visualized. In **c**, **d** the normalized displacement components and the displacement magnitude are depicted on the surface for selected angles. The radial dependencies of the displacement functions are plotted in **e**–**h**. Here, **e**, **g** are w.r.t. the permanent magnet, **f**, **h** w.r.t. the linear one. **a** Permanent magnetic sphere. **b** Linear-magnetic sphere. **c** Permanent magnetic sphere. **d** Linear-magnetic sphere. **e** Radial displacement component $\tilde{u}_r^{(\mathrm{I})}$. **f** Radial displacement component $\tilde{u}_r^{(\mathrm{II})}$. **g** Polar displacement component $\tilde{u}_\vartheta^{(\mathrm{I})}$. **h** Polar displacement component $\tilde{u}_\vartheta^{(\mathrm{II})}$

the magnitude of the largest (and smallest) strain cannot be read off directly. Rather, the eigenvalue problem has to be solved to acquire the principal strains Λ_i of the system. This yields:

$$\Lambda_{1/2} = \frac{1}{2}\left[\varepsilon_{rr} + \varepsilon_{\vartheta\vartheta} \pm \sqrt{\varepsilon_{rr}^2 + \varepsilon_{\vartheta\vartheta}^2 + 4\varepsilon_{r\vartheta}^2 - 2\varepsilon_{rr}\varepsilon_{\vartheta\vartheta}}\right], \quad \Lambda_3 = \varepsilon_{\varphi\varphi}. \tag{7.3}$$

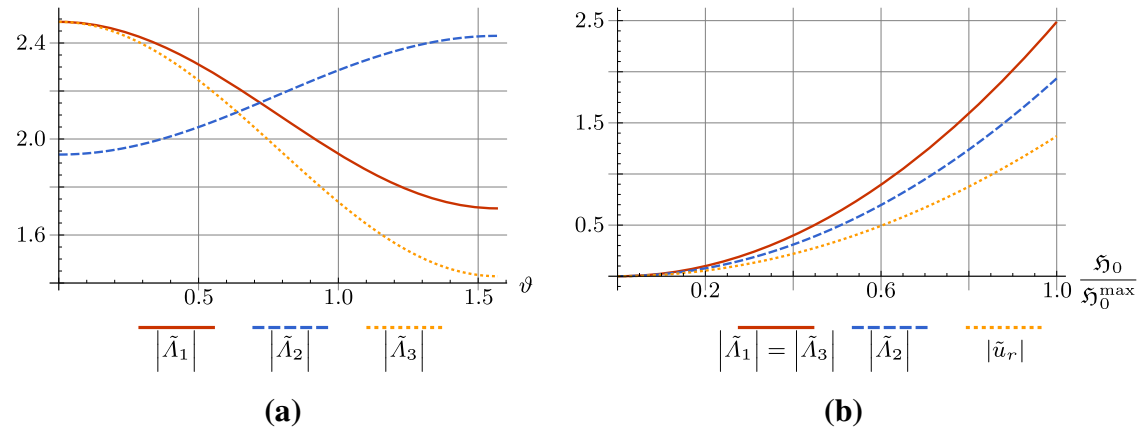

Fig. 7 Normalized principal strains $\tilde{\Lambda}_i$ for the *linear-magnetic* sphere. In **a**, the strains are plotted against the polar angle for a fixed $\mathfrak{H}_0$ on the surface. In **b**, the strains and the radial displacement component are plotted against the magnitude of the external field at the pole $\vartheta = 0$, $\tilde{r} = 1$. The ratios $\lambda/\mu = 1.27$ and $\mu_\mathrm{r} = 100$ were used. **a** Principal strains on the surface of a spherical linear magnet. **b** Principal strains and the radial displacement component of the linear-magnetic sphere

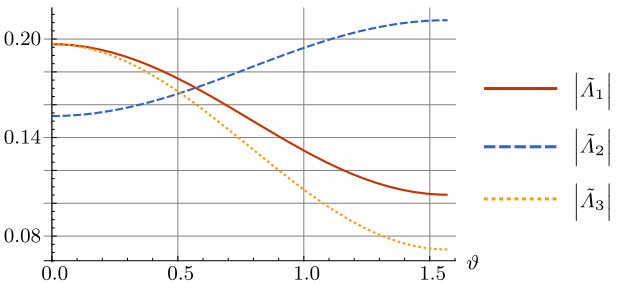

Fig. 8 Normalized principal strains $\tilde{\Lambda}_i$ on the surface of the *permanent magnetic* sphere. The ratio $\lambda/\mu = 1.27$ was employed. For normalization $\Lambda_i^{(\mathrm{I})} = \hat{\sigma}^{(\mathrm{I})}\mu^{-1}\tilde{\Lambda}_i^{(\mathrm{I})}$ was used

Note that the strains $\varepsilon_{\vartheta\varphi}$ and $\varepsilon_{\varphi r}$ vanish since $u_\varphi = 0$. The magnitude of all strain tensor components is governed by the factors $\hat{\sigma}^{(\mathrm{I/II})}\mu^{-1}$. Therefore, the magnitude of the principal strains is determined by these factors as well. The normalization $\Lambda_i^{(\mathrm{I/II})} = \hat{\sigma}^{(\mathrm{I/II})}\mu^{-1}\tilde{\Lambda}_i^{(\mathrm{I/II})}$ is employed. We are interested in the principal strains w.r.t. the initial magnetization process and the remanent eigenstrains once the external field is deactivated.

The normalized principal strains on the linear-magnetic sphere's surface with $\mu_\mathrm{r} = 100$ are shown in Fig. 7. The principal strains of largest magnitude are located at the poles. Therefore, the strains due to magnetization are analyzed there. In our physical model, all resulting strains have the same normalization factor, i.e., $\hat{\sigma}^{(\mathrm{II})}\mu^{-1} = \mu_0\mathfrak{H}_0^2\mu^{-1}$, which is quadratic in the magnitude of the external field. Hence, the strain functions are quadratic in the magnitude of the external field. This can also be seen in the figure.

Often a ratio of the form $(\ell-\ell_0)/\ell_0$ is measured in order to analyze the magnetostriction effect, where ℓ and ℓ_0 denote some characteristic deformed and undeformed length measure, respectively. However, such a ratio can underestimate the true size of the strains. To show this, consider the ratio u_r/R at the pole. In order to compare this ratio with the normalized principle stresses we scale by $\hat{\sigma}^{(\mathrm{II})}\mu^{-1}$. The resulting normalized ratio is equal to $\tilde{u}_r$. Therefore, the normalized radial displacement is also visualized in Fig. 7 at the pole $\vartheta = 0$, $\tilde{r} = 1$ for a variation of the external field. As can be seen, the largest strain value is almost 100 % larger than this (potentially measured) value. Of course, the quadratic strain behavior is only valid for the initial phase of the magnetization process, because a linear model was employed, where $\mu_\mathrm{r} = \text{const}$, cf., Fig. 1. For higher amplitudes of the external field, the model has to be extended, e.g., $\mu_\mathrm{r}(\mathfrak{H})$ has to be prescribed.

The principal strains of the remanent magnetic problem can be seen in Fig. 8. The resulting graph is similar to the previously shown paramagnetic case, albeit with a difference in magnitude and polar angle dependency. Due to the symmetry of the displacements w.r.t. the equatorial plane, the principal strains are symmetric to this plane as well. The same holds for the mechanical stresses.

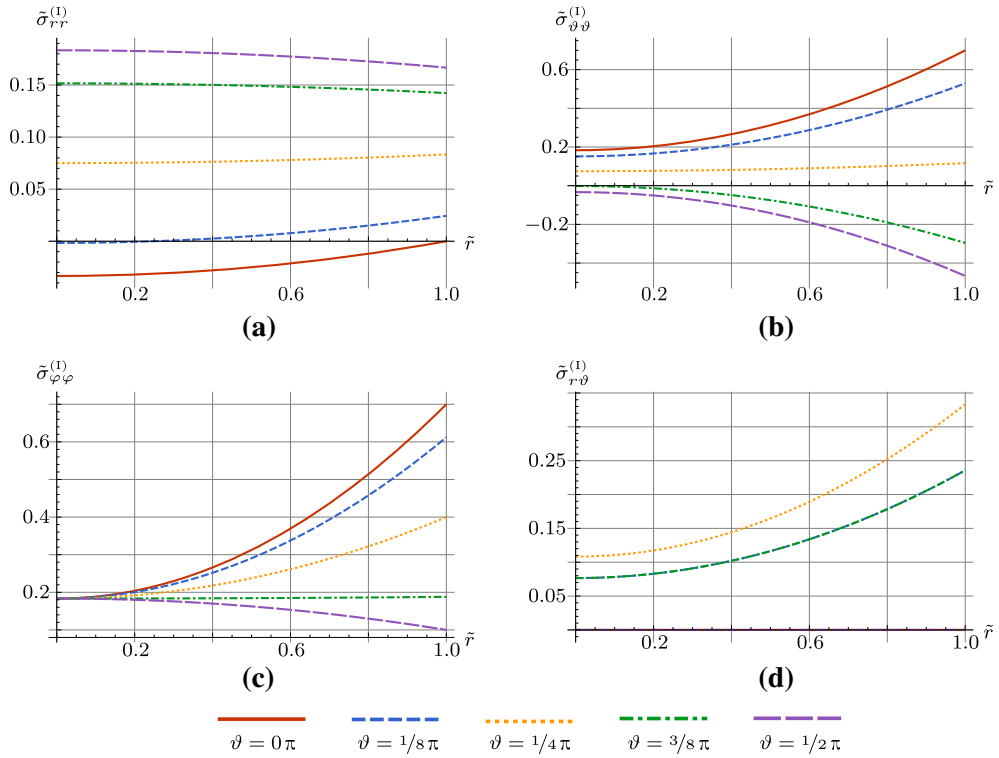

Fig. 9 Stresses in a spherical magnet due to the remanent magnetic field for selected polar angles, normalized by $\hat{\sigma}^{(\mathrm{I})}$. For visualization, the ratio $\lambda/\mu = 1.27$ was used to represent steel. **a** Radial stress $\tilde{\sigma}^{(\mathrm{I})}_{rr}(\tilde{r}, \vartheta)$. **b** Polar stress $\tilde{\sigma}^{(\mathrm{I})}_{\vartheta\vartheta}(\tilde{r}, \vartheta)$. **c** Azimuthal stress $\tilde{\sigma}^{(\mathrm{I})}_{\varphi\varphi}(\tilde{r}, \vartheta)$. **d** Shear stress $\tilde{\sigma}^{(\mathrm{I})}_{r\vartheta}(\tilde{r}, \vartheta)$

7.4 Stresses

The scale and dimension of the stresses in Eq. (6.8) are governed by the factors $\hat{\sigma}^{(\mathrm{I/II})}$. This motivates the normalizations $\sigma_{ij}^{(\mathrm{I/II})} = \hat{\sigma}^{(\mathrm{I/II})}\tilde{\sigma}_{ij}^{(\mathrm{I/II})}$. The normalized stresses are visualized in Figs. 9 and 10. It can be seen there that the boundary conditions are satisfied. For example, at the poles we have $\boldsymbol{f}^{\mathrm{L}}_{I\,(\mathrm{I/II})}(\tilde{r} = 1, \vartheta = 0) = \boldsymbol{0}$. Therefore, we must have $\tilde{\sigma}^{(\mathrm{I/II})}_{rr}(\tilde{r} = 1, \vartheta = 0) = \tilde{\sigma}^{(\mathrm{I/II})}_{r\vartheta}(\tilde{r} = 1, \vartheta = 0) = 0$, as can clearly be seen in the graphs. The solutions of the linear problems of elasticity satisfy the boundary conditions; therefore, they are complete and unique (up to rigid body modifications).

In the problem of the remanent magnetic sphere, the azimuthal stress and the nonvanishing shear stress are always positive, cf., Fig. 9. The same holds for paramagnetic media in the magnetization process, as can be seen in Fig. 10, where $\mu_{\mathrm{r}} = 100$. In both demonstrated problems, the polar and the azimuthal stresses are considerably higher in absolute value than the other stress components. In general, this does not hold in case of diamagnetic media.

For both problems, there are noteworthy symmetry relations of the stress functions w.r.t. the polar angle. We find that the functions:

$$P_2(x)\,, \quad \cot\vartheta\,\frac{\mathrm{d}P_2(x)}{\mathrm{d}\vartheta}\,, \quad \text{and} \quad \frac{\mathrm{d}^2 P_2}{\mathrm{d}\vartheta^2}$$

are even functions w.r.t. the angle $\vartheta = \pi/2$, e.g., $P_2(\cos(\pi/2 + \alpha)) = P_2(\cos(\pi/2 - \alpha))$. Also, $\mathrm{d}P_2(x)/\mathrm{d}\vartheta$ is an odd function w.r.t. this angle. Therefore, the stresses

$$\sigma_{rr}^{(\mathrm{I/II})}(\tilde{r}, \vartheta)\,, \quad \sigma_{\vartheta\vartheta}^{(\mathrm{I/II})}(\tilde{r}, \vartheta)\,, \quad \sigma_{\varphi\varphi}^{(\mathrm{I/II})}(\tilde{r}, \vartheta)$$

are even functions and $\sigma_{r\vartheta}^{(\mathrm{I/II})}(\tilde{r}, \vartheta)$ are odd functions w.r.t. $\vartheta = \pi/2$. For this reason, the stresses in the Figs. 9 and 10 are only plotted for angles $\vartheta \in [0, \pi/2]$. Moreover, $\mathrm{d}P_2(x)/\mathrm{d}\vartheta$ constitutes an even function w.r.t. the angle $\vartheta = \pi/4$. Therefore, we have, for example, $\tilde{\sigma}_{r,\vartheta}^{(\mathrm{I/II})}(\tilde{r}, \vartheta = \pi/8) = \tilde{\sigma}_{r,\vartheta}^{(\mathrm{I/II})}(\tilde{r}, \vartheta = 3\,\pi/8)$. This can be seen in the figures.

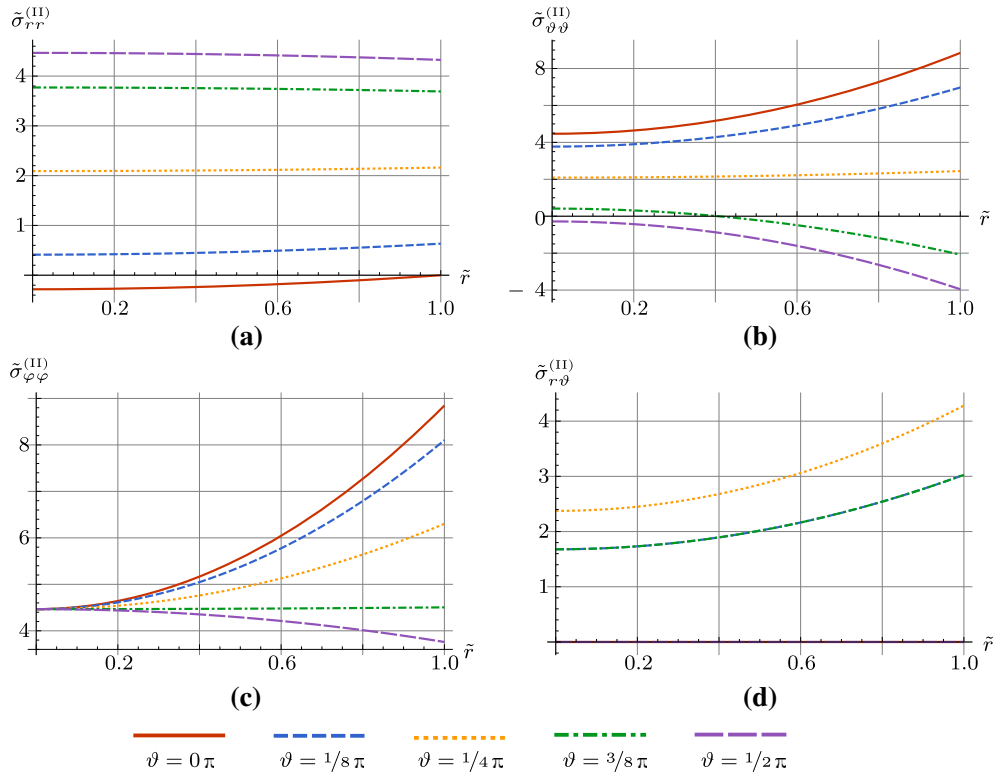

Fig. 10 Stresses in the linear-magnetic sphere due to an external field for selected polar angles, normalized by $\hat{\sigma}^{(\mathrm{II})}$. For visualization, the values $\lambda/\mu = 1.27$ and $\mu_\mathrm{r} = 100$ were chosen. **a** Radial stress $\tilde{\sigma}^{(\mathrm{II})}_{rr}(\tilde{r}, \vartheta)$. **b** Polar stress $\tilde{\sigma}^{(\mathrm{II})}_{\vartheta\vartheta}(\tilde{r}, \vartheta)$. **c** Azimuthal stress $\tilde{\sigma}^{(\mathrm{II})}_{\varphi\varphi}(\tilde{r}, \vartheta)$. **d** Shear stress $\tilde{\sigma}^{(\mathrm{II})}_{r\vartheta}(\tilde{r}, \vartheta)$

Given these stress functions, one may be interested in an equivalent one-dimensional stress measure and its magnitude. We start from the VON MISES equivalent stress concept for ductile media:

$$2\sigma^2_{\mathrm{vM}} = (\sigma_{rr} - \sigma_{\vartheta\vartheta})^2 + (\sigma_{rr} - \sigma_{\varphi\varphi})^2 + (\sigma_{\vartheta\vartheta} - \sigma_{\varphi\varphi})^2 + 6\sigma^2_{r\vartheta}.$$

Since each stress component is linear in the factors $\hat{\sigma}^{(\mathrm{I/II})}$, the equivalent stress can also be normalized by $\sigma^{(\mathrm{I/II})}_{\mathrm{vM}} = \hat{\sigma}^{(\mathrm{I/II})}\tilde{\sigma}^{(\mathrm{I/II})}_{\mathrm{vM}}$. For a spherical permanent magnet with a remanence of one tesla, this factor is approximately one megapascal. For the problem of a linear-magnetic sphere, this factor varies with the magnitude of the applied external field. Consider the normalized equivalent VON MISES stresses shown in Fig. 11. For the permanent magnet, the function $\tilde{\sigma}^{(\mathrm{I})}_{\mathrm{vM}}$ is of order one, independent of the remanent field. Realistic variations of λ/μ do not change this property. Hence, for this problem the magnitude of the equivalent stress on the surface is approximately given by the factor $\hat{\sigma}^{(\mathrm{I})}$.

For a linear magnet in an external field, the situation is more complex. The stress amplitude varies with the factor $\hat{\sigma}^{(\mathrm{II})}$ and with relative permeability μ_r. For example, for $\mu_\mathrm{r} = 100$, $\tilde{\sigma}^{(\mathrm{II})}_{\mathrm{vM}}$ is of order ten. Therefore, one needs to take care when examining the state of stress in magnetization processes. However, the stresses are limited w.r.t. variation of μ_r. This can be seen by studying the limits of the sources, i.e., the LORENTZ traction limits in Eq. (7.2), examined in Sect. 7.1. Also, in diamagnetic problems, one can show that the maximum equivalent stress values are located at the center of the deformed sphere. Note that if the considered magnet is too brittle, the VON MISES equivalent stress concept might not be applicable. In this case, the hypothesis of RANKINE could be applicable, which considers the highest principal stress value.

8 Conclusions

After a brief summary of the governing equations and constitutive laws of magnetostatics and elasticity, we computed the magnetic force on spherical bodies for two cases. First, we considered a permanent magnetic sphere and second, a linear-magnetic sphere in an external field.

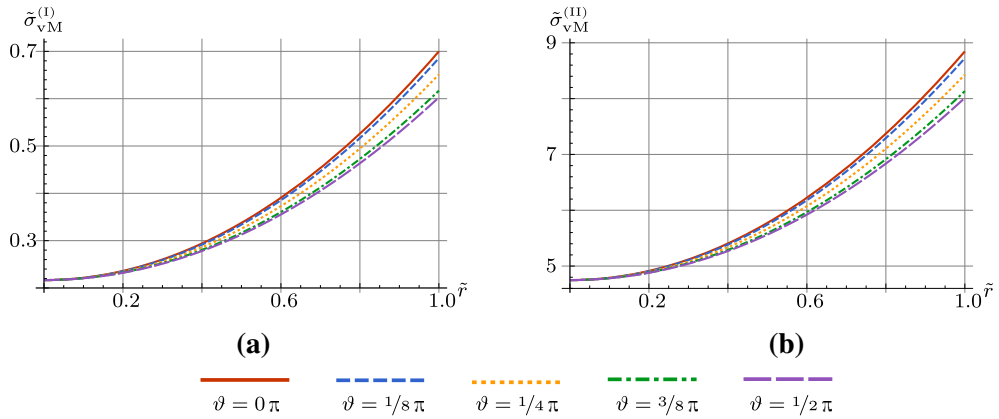

Fig. 11 VON MISES equivalent stress for both problems. For visualization, the values $\lambda/\mu = 1.27$ and $\mu_\mathrm{r} = 100$ were chosen. **a** Sphere with remanent magentic field, normalized by $\hat{\sigma}^{(\mathrm{I})}$. **b** Linear-magnetic sphere in an external field, normalized by $\hat{\sigma}^{(\mathrm{II})}$

We started by reviewing the magnetic fields of the problems and computed the individual body and surface LORENTZ force densities with the theory detailed in [5]. In both cases, the LORENTZ force model yielded vanishing electromagnetic body forces and nonvanishing electromagnetic surface tractions. In the considered problems, the tractions possess both radial as well as polar components—hence the loadings are not spherically symmetric. This seems noteworthy because some authors obtained purely normal traction loadings, see [1,12].

The computed LORENTZ tractions are azimuthally symmetric, therefore, the analytic solution of HIRAMATSU and OKA for the LAMÉ-NAVIER equations was applied. It was shown that the boundary conditions of our problems in terms of their general solution are suitably expandable in (modified) FOURIER-LEGENDRE series. The components of the force densities in both problems show the same dependence on the polar angle. Therefore, the FOURIER-LEGENDRE expansions possess the same mathematical structure and can be treated simultaneously in the elasticity problem. Examination of the jump condition of linear momentum led to an infinite linear algebraic system. However, due to the structure of the traction, only a few coefficients of the series do not vanish. Hence, the series becomes finite and the displacements and stresses can be stated in closed form.

During the analysis it was shown that the occurring displacements in technically relevant situations are small, as to be expected. The displacement fields possess symmetry w.r.t. the equatorial plane. It is interesting to note that even though the loading is azimuthally symmetric, the displacements at the poles and the equator are not maximum in magnitude. This property is independent of the material parameters and, in case of the linear sphere, of the external field strength. Nonetheless, the exact polar angles of largest displacement on the surface are determined by these parameters.

Remarkably, the largest total change in diameter w.r.t. the undeformed sphere can be observed either in the equatorial plane or at the axis of symmetry. Often, the strains in a system are estimated by dividing the largest measured length change with its reference length. Due to the fact that the displacements are not spherically symmetric, there are shear strains w.r.t. the spherical coordinate system. The largest strains of the problems were computed by solving the eigenvalue problem. In the problems examined above, the largest principal strain is about 100% larger than the simple strain estimation.

Analysis of the stresses showed that the circumferential stresses are largest in magnitude. Therefore, the equivalent stress measures are primarily governed by these. For the permanent magnetic sphere, it was shown that the magnitude of largest stress can be well estimated with the factor $\hat{\sigma}^{(\mathrm{I})} = \mu_0 M_0^2$. However, in the case of the linear-magnetic sphere, the largest stress cannot solely be estimated by the factor $\hat{\sigma}^{(\mathrm{II})} = \mu_0 \mathfrak{H}_0^2$. This is due to the fact that the amplifying functions for the linear-magnetic case are not of order one but rather strongly depend upon the value of relative permeability μ_r. In the example illustrated above, the magnitude of amplifying function of the equivalent stress is about ten.

In conclusion, the spherical magnetostriction problems were solved analytically in closed form. The solutions are firmly based upon the LORENTZ force concept. In the future, these analytical solutions may serve for validation of numerical magentostriction solvers that also incorporate this force concept.

Table 1 MAXWELL'S equations and equations of non-free electric charge

	Regular points	Singular points
FARADAY'S law of induction	$\frac{\partial \boldsymbol{B}}{\partial t} + \nabla \times \boldsymbol{E} = \boldsymbol{0}$	$-[\![\boldsymbol{B}]\!] w_\perp + \boldsymbol{n} \times [\![\boldsymbol{E}]\!] = \boldsymbol{0}$
GAUSS'S law for magnetism	$\nabla \cdot \boldsymbol{B} = 0$	$\boldsymbol{n} \cdot [\![\boldsymbol{B}]\!] = 0$
AMPÉRE'S circuital law	$\frac{\partial \mathfrak{D}}{\partial t} - \nabla \times \mathfrak{H} = -\boldsymbol{J}^{\mathrm{f}}$	$-[\![\mathfrak{D}]\!] w_\perp - \boldsymbol{n} \times [\![\mathfrak{H}]\!] = -\boldsymbol{J}_I^{\mathrm{f}}$
GAUSS'S law	$\nabla \cdot \mathfrak{D} = q^{\mathrm{f}}$	$\boldsymbol{n} \cdot [\![\mathfrak{D}]\!] = q_I^{\mathrm{f}}$
Non-free electric current	$-\frac{\partial \boldsymbol{P}}{\partial t} - \nabla \times \boldsymbol{M} = -\boldsymbol{J}^{\mathrm{r}}$	$[\![\boldsymbol{P}]\!] w_\perp - \boldsymbol{n} \times [\![\boldsymbol{M}]\!] = -\boldsymbol{J}_I^{\mathrm{r}}$
Non-free electric charge	$-\nabla \cdot \boldsymbol{P} = q^{\mathrm{r}}$	$-\boldsymbol{n} \cdot [\![\boldsymbol{P}]\!] = q_I^{\mathrm{r}}$

A Maxwell's equations

In problems of continuum physics, steep gradients of fields may occur within the body. These are modeled by so-called singular surfaces at which the physical fields become discontinuous. These surfaces are often referred to as *interfaces* and points on them as *singular*. In these points, the differential equation of the surrounding (continuous) bulk do not apply. This also holds in the theory of electromagnetism, i.e., MAXWELL'S regular equations do not hold everywhere. The governing equations can be derived from balance equation in a rational manner, as described in [17]. In a domain containing a singular surface, the balances of electric charge and magnetic flux are analyzed by virtue of generalized integral and flux theorems. Limit processes yield equations for singular points that are particularly helpful for characterizing boundary and transition conditions.

The results of this approach are compiled in Table 1. Interface densities are marked by the index I. The symbol $w_\perp$ denotes the normal component of the interface velocity, i.e., $\boldsymbol{n} \cdot \boldsymbol{w}$. Double brackets denote the jump operator, which is defined as follows. An interface I dissects a domain in two regions, Ω_- and Ω_+. Let χ be a continuous field in the domains $\Omega_\pm$. The jump of this field is then

$$[\![\chi(\boldsymbol{x}_I, t)]\!] := \chi_+(\boldsymbol{x}_I, t) - \chi_-(\boldsymbol{x}_I, t) \,, \quad \chi_\pm(\boldsymbol{x}_I, t) := \lim_{\boldsymbol{x}_\pm \to \boldsymbol{x}_I} \chi(\boldsymbol{x}_\pm) \,, \quad \boldsymbol{x}_\pm \in \Omega_\pm \,, \quad \boldsymbol{x}_I \in I. \tag{A.1}$$

Of course, there is some arbitrariness which side is referred to as $+$ or $-$. However, this causes no problems when applying the chosen definition everywhere. In this paper, we employ the convention that $-$ and $+$ refer to the inside and outside of the spheres, respectively. The direction of the normal vector is defined to point from the $-$ into the $+$ domain. In this paper, $\boldsymbol{n} = \boldsymbol{e}_r$.

In the context of continuum physics, the symbols in the equations of Table 1 are identified in this paper as follows. The fields $\boldsymbol{E}$ and $\boldsymbol{B}$ are referred to as the electric field and the magnetic flux density, respectively. They are not independent of each other. Rather, they are parts of a four-dimensional space-time tensor. The same holds for the fields $\mathfrak{D}$ and $\mathfrak{H}$, which are called charge potential in matter and current potential in matter, respectively. Their definition is based on the balance of free electric current. Moreover, the quantity q^{f} denotes the free electric charge and $\boldsymbol{J}^{\mathrm{f}}$ the free electric current. If the index "f" is exchanged with "r", densities w.r.t. the balance of bound electric charge will result. This balance gives rise to potential fields $\boldsymbol{P}$ and $\boldsymbol{M}$, which are properly called bound charge potential and bound current potential, respectively. In this work, they are referred to by their more common names, i.e., polarization and (MINKOWSKI) magnetization. Since the balances of total, free, and bound electric charge are not independent of each other, the following relations hold:

$$q = q^{\mathrm{f}} + q^{\mathrm{r}} \,, \quad \boldsymbol{J} = \boldsymbol{J}^{\mathrm{f}} + \boldsymbol{J}^{\mathrm{r}} \,, \quad \mathfrak{H} = \tfrac{1}{\mu_0} \boldsymbol{B} - \boldsymbol{M} \,, \quad \mathfrak{D} = \varepsilon_0 \boldsymbol{E} + \boldsymbol{P}. \tag{A.2a}$$

In these formulae, the MAXWELL-LORENTZ aether relations were incorporated. They connect the potentials of total electric charge and of total electric current with the fields $\boldsymbol{E}$ and $\boldsymbol{B}$. It can often be beneficial to decompose the free electric current density into a diffusive ($\boldsymbol{j}^{\mathrm{f}}$) and a non-diffusive part ($q^{\mathrm{f}} \boldsymbol{v}$), that can loosely be referred to as non-convective and convective electric current densities, respectively:

$$\boldsymbol{J}^{\mathrm{f}} = q^{\mathrm{f}} \boldsymbol{v} + \boldsymbol{j}^{\mathrm{f}} \,, \quad \boldsymbol{J}_I^{\mathrm{f}} = q_I^{\mathrm{f}} \boldsymbol{v}_I + \boldsymbol{j}_I^{\mathrm{f}}. \tag{A.2b}$$

Here, $\boldsymbol{v}$ denotes the barycentric velocity of a medium. A theory of mixtures in context of electromagnetism is detailed in [5]. For a review of continuum electromagnetism see [8].

B Lorentz force model

There is no general consensus on the precise form of the electromagnetic coupling in the literature. This was already stated in [17, p. 686], where it is argued that there are *laws of interaction* that cannot be stated in a general manner. For this reason, some authors avoid a specific definition during thermodynamics based investigations, for example in [8]. However, there is general agreement that all coupling models coincide when magnetization and polarization vanish. That is, when $q = q^{\mathrm{f}}$ and $\boldsymbol{J} = \boldsymbol{J}^{\mathrm{f}}$ there holds:

$$\boldsymbol{f}^{\mathrm{L}} = q^{\mathrm{f}}\boldsymbol{E} + \boldsymbol{J}^{\mathrm{f}} \times \boldsymbol{B}. \tag{B.1}$$

The authors follow [10] and model the force coupling in regular points with *total* densities q and $\boldsymbol{J}$ by:

$$\boldsymbol{f}^{\mathrm{L}} = q\boldsymbol{E} + \boldsymbol{J} \times \boldsymbol{B}. \tag{B.2}$$

The basic concept of this equation is the idea that all charges and currents induce forces independently of their nature, i.e., in this context there is no difference between free and bound charges and currents. By using the relations of Table 1 and Eq. (A.2), this force model can be rewritten to show all specific contributions:

$$\boldsymbol{f}^{\mathrm{L}} = (q^{\mathrm{f}} - \nabla \cdot \boldsymbol{P})\boldsymbol{E} + \left(q^{\mathrm{f}}\boldsymbol{v} + \boldsymbol{j}^{\mathrm{f}} + \frac{\partial \boldsymbol{P}}{\partial t} + \nabla \times \boldsymbol{M}\right) \times \boldsymbol{B}. \tag{B.3a}$$

It is possible to find the identity

$$\boldsymbol{f}^{\mathrm{L}} = \nabla \cdot \boldsymbol{m} - \frac{\partial \boldsymbol{g}}{\partial t} \quad \text{where} \quad \boldsymbol{m} = -\tfrac{1}{2}\left(\epsilon_0 \boldsymbol{E}^2 + \tfrac{1}{\mu_0}\boldsymbol{B}^2\right)\mathbf{1} + \epsilon_0 \boldsymbol{E} \otimes \boldsymbol{E} + \tfrac{1}{\mu_0}\boldsymbol{B} \otimes \boldsymbol{B}, \quad \boldsymbol{g} = \epsilon_0 \boldsymbol{E} \otimes \boldsymbol{B}. \tag{B.3b}$$

Based on this identity, a volumetric limit process of the balance of linear momentum yields the following corresponding surface traction:

$$\boldsymbol{f}_I^{\mathrm{L}} = q_I \langle \boldsymbol{E} \rangle + \boldsymbol{J}_I \times \langle \boldsymbol{B} \rangle . \tag{B.3c}$$

In this equation, mean values were used. The mean value of a field is defined analogously to the jump, *viz.*:

$$\langle \chi(\boldsymbol{x}_I, t) \rangle := \tfrac{1}{2}[\chi_+(\boldsymbol{x}_I, t) + \chi_-(\boldsymbol{x}_I, t)], \quad \chi_\pm(\boldsymbol{x}_I, t) := \lim_{\boldsymbol{x}_\pm \to \boldsymbol{x}_I} \chi(\boldsymbol{x}_\pm), \quad \boldsymbol{x}_\pm \in \Omega_\pm, \quad \boldsymbol{x}_I \in I. \tag{B.3d}$$

For the surface traction, it also possible to employ Table 1 and formulae analogous to Eq. (A.2) in order to show specific contributions:

$$\boldsymbol{f}_I^{\mathrm{L}} = (q_I^{\mathrm{f}} - \boldsymbol{n} \cdot [\![\boldsymbol{P}]\!]) \langle \boldsymbol{E} \rangle + (q_I^{\mathrm{f}} \boldsymbol{v}_I + \boldsymbol{j}_I^{\mathrm{f}} - w_\perp [\![\boldsymbol{P}]\!] + \boldsymbol{n} \times [\![\boldsymbol{M}]\!]) \times \langle \boldsymbol{B} \rangle . \tag{B.3e}$$

The precise steps of this derivation are detailed in [5].

C Balance of linear momentum for regular and singular points

In regular points, the balance of mechanical linear momentum can be denoted by:

$$\frac{\partial}{\partial t}(\rho \boldsymbol{v}) + \nabla \cdot (\rho \boldsymbol{v} \otimes \boldsymbol{v} - \boldsymbol{\sigma}) = \rho \boldsymbol{f} + \boldsymbol{f}^{\mathrm{L}}. \tag{C.1}$$

Note that the source of body forces is decomposed into the classical density $\rho \boldsymbol{f}$, which is proportional to mass, and an electromagnetic source $\boldsymbol{f}^{\mathrm{L}}$. The former density can be regarded as gravity, the latter as the LORENTZ force. Here, $\boldsymbol{\sigma}$ denotes the pure *mechanical* stress tensor. By using the abbreviation

$$\nabla_I := \mathbf{1}_I \cdot \nabla \quad \text{where} \quad \mathbf{1}_I = \mathbf{1} - \boldsymbol{n} \otimes \boldsymbol{n}, \tag{C.2}$$

the balance for points on a singular surface can be denoted by:

$$\frac{\partial}{\partial t}(\rho_I \boldsymbol{v}_I) - \boldsymbol{w} \cdot \nabla_I \otimes (\rho_I \boldsymbol{v}_I) + \nabla_I \cdot (\rho_I \boldsymbol{v}_I \otimes \boldsymbol{v}_I - \boldsymbol{\sigma}_I) - 2H\boldsymbol{n} \cdot \boldsymbol{\sigma}_I = \boldsymbol{n} \cdot [\![\boldsymbol{\sigma} + \rho(\boldsymbol{w} - \boldsymbol{v}) \otimes \boldsymbol{v}]\!] + \rho_I \boldsymbol{f}_I + \boldsymbol{f}_I^{\mathrm{L}}, \tag{C.3}$$

where the mean curvature is defined by $\nabla_I \cdot \boldsymbol{n} = -2H$. In this formula, there are also surface source densities of gravity and electromagnetism. If the singular surface is without intrinsic structure, this balance significantly simplifies and reads:

$$\boldsymbol{n} \cdot [\![\boldsymbol{\sigma} + \rho(\boldsymbol{w} - \boldsymbol{v}) \otimes \boldsymbol{v}]\!] = -\boldsymbol{f}_I^{\mathrm{L}}. \tag{C.4}$$

The LORENTZ surface traction is not (purely) intrinsic to the interface. Rather this density is closely related to regular field values in close proximity of the surface as detailed in Eq. (B.3e). For thorough reviews of the balance equations for regular and singular points see [2,14,15].

D Some formulas regarding Legendre polynomials

The polynomials $P_n(x)$ satisfy LEGENDRE'S differential equation,

$$\frac{\mathrm{d}}{\mathrm{d}x}\left[(1-x^2)\frac{\mathrm{d}P_n(x)}{\mathrm{d}x}\right]+n(n+1)P_n(x)=0, \tag{D.1}$$

where $x\in[-1,1]$. The polynomials can be computed by virtue of RODRIGUES' formula:

$$P_n(x)=\frac{1}{2^n n!}\frac{\mathrm{d}^n}{\mathrm{d}x^n}[(x^2-1)^n] \quad\Rightarrow\quad P_1(x)=1\,,\quad P_2(x)=x\,,\quad P_3(x)=\tfrac{1}{2}(3x^2-1)\;\ldots \tag{D.2}$$

In context of the analyzed problems, the following relations of orthogonality are helpful for series expansions:

$$\int_{x=-1}^{1} P_m(x)P_n(x)\,\mathrm{d}x=\frac{2}{2m+1}\delta_{nm}\,,\qquad \int_{x=-1}^{1}(1-x^2)\frac{\mathrm{d}P_m(x)}{\mathrm{d}x}\frac{\mathrm{d}P_n(x)}{\mathrm{d}x}\,\mathrm{d}x=\frac{2m(m+1)}{2m+1}\delta_{nm}. \tag{D.3}$$

The first relation is common knowledge, the second can be proved as follows.

Proof Form an integral of zero value:

$$\int_{x=-1}^{1}\frac{\mathrm{d}}{\mathrm{d}x}\left[(1-x^2)\frac{\mathrm{d}P_m(x)}{\mathrm{d}x}P_n(x)\right]\mathrm{d}x=\left[(1-x^2)\frac{\mathrm{d}P_m(x)}{\mathrm{d}x}P_n(x)\right]_{x=-1}^{1}=0. \tag{D.4}$$

Use integration by parts for this integral and LEGENDRE'S equation:

$$\begin{aligned}0&=\int_{x=-1}^{1}\frac{\mathrm{d}}{\mathrm{d}x}\left[(1-x^2)\frac{\mathrm{d}P_m(x)}{\mathrm{d}x}\right]P_n(x)\,\mathrm{d}x+\int_{x=-1}^{1}(1-x^2)\frac{\mathrm{d}P_m(x)}{\mathrm{d}x}\frac{\mathrm{d}P_n(x)}{\mathrm{d}x}\,\mathrm{d}x\\&=-m(m+1)\int_{x=-1}^{1}P_m(x)P_n(x)\,\mathrm{d}x+\int_{x=-1}^{1}(1-x^2)\frac{\mathrm{d}P_m(x)}{\mathrm{d}x}\frac{\mathrm{d}P_n(x)}{\mathrm{d}x}\,\mathrm{d}x.\end{aligned} \tag{D.5}$$

Insertion of orthogonality relation $(\mathrm{D.3})_1$ yields the formula. □

By noting that $\mathrm{d}P_n(x)/\mathrm{d}\vartheta=-\sqrt{1-x^2}\,\mathrm{d}P_n(x)/\mathrm{d}x$, formula $(\mathrm{D.3})_2$ is equivalent to the useful relation

$$\int_{x=-1}^{1}\frac{\mathrm{d}P_m(x)}{\mathrm{d}\vartheta}\frac{\mathrm{d}P_n(x)}{\mathrm{d}\vartheta}\,\mathrm{d}x=\frac{2m(m+1)}{2m+1}\delta_{nm}. \tag{D.6}$$

References

1. Brown, W.F.: Magnetoelastic Interactions, Springer Tracts in Natural Philosophy, vol. 9. Springer, Berlin (1966)
2. Dziubek, A.: Equations for two-phase flows: a primer. arXiv:1101.5732 (2011)
3. Eringen, A.C., Maugin, G.A.: Electrodynamics of Continua I: Foundations and Solid Media. Springer, Berlin (2012)
4. Fitzpatrick R.: Leture notes: Classical electromagnetism: an intermediate level course. University of Texas, Austin (2014)
5. Guhlke, C.: Theorie der elektrochemischen Grenzfläche. Ph.D. thesis, Technische Universität Berlin (2015)
6. Hiramatsu, Y., Oka, Y.: Determination of the tensile strength of rock by a compression test of an irregular test piece. Int. J. Rock Mech. Min. Sci. Geomech. Abstr. **3**(2), 89–90 (1966)
7. Jackson, J.D.: Classical Electrodynamics, 2nd edn. Wiley, Hoboken (1975)
8. Kovetz, A.: Electromagnetic Theory. Oxford University Press, Oxford (2000)
9. Love, A.E.H.: A Treatise on the Mathematical Theory of Elasticity. Dover Books on Engineering and Engineering Physics. Dover Publications, Mineola (1944)
10. Müller, I.: Thermodynamics. Interaction of Mechanics and Mathematics Series. Pitman, Boston (1985)
11. Müller, W.H.: An Expedition to Continuum Theory. Solid Mechanics and Its Applications Series. Springer, Berlin (2014)

12. Raikher, Y.L., Stolbov, O.V.: Deformation of an ellipsoidal ferrogel sample in a uniform magnetic field. J. Appl. Mech. Tech. Phys. **46**(3), 434–443 (2005)
13. Rinaldi, C., Brenner, H.: Body versus surface forces in continuum mechanics: is the Maxwell stress tensor a physically objective Cauchy stress? Phys. Rev. E **65**(3), 036615 (2002)
14. Slattery, J.C., Sagis, L., Oh, E.S.: Interfacial Transport Phenomena. Springer, Berlin (2007)
15. Steinmann, P.: On boundary potential energies in deformational and configurational mechanics. J. Mech. Phys. Solids **56**(3), 772–800 (2008)
16. Stratton, J.A.: Electromagnetic Theory. McGraw-Hill, New York (1941)
17. Truesdell, C.A., Toupin, R.: The classical field theories. In: Handbuch der Physik, Bd. III/1, pp. 226–793; appendix, pp. 794–858. Springer, Berlin (1960). With an appendix on tensor fields by J. L. Ericksen
18. Wei, X.X., Wang, Z.M., Xiong, J.: The analytical solutions for the stress distributions within elastic hollow spheres under the diametrical point loads. Arch. Appl. Mech. **85**(6), 817–830 (2015)